ChemPubSoc Europe

DOI: 10.1002/slct.201803685

Chemistry SELECT Reviews

Organic & Supramolecular Chemistry

Recent Developments in Fluorometric and Colorimetric Chemodosimeters Targeted towards Hydrazine Sensing: Present Success and Future Possibilities

Saikat Kumar Manna,[a] Ankita Gangopadhyay,[b] Kalipada Maiti,[b] Sanchita Mondal,[b] and Ajit Kumar Mahapatra*[b]

Recently, the design, synthesis and development of chemodosimeters for hydrazine with high selectivity and sensitivity has attracted tremendous attention due to its major contributions to human health and disease including applications in various platforms. In this review, we recapitulate different strategies for the design of reaction-based colorimetric and fluorometric probes for the detection of hydrazine and their applications in hydrazine sensing in living systems. The sensing strategies for hydrazine have been divided into six categories: (a) cleavage of the acetoxy group; (b) the nucleophilic addition-elimination on keto ester; (c) the nucleophilic substitution-elimination to tandem cyclization on halo-ester; (d) the nucleophilic addition reaction to phthalimide derivative to phthalhydrazide; (e) the chemical displacement of active methylene compound to hydrazone derivative and (f) Other different approaches. Additionally, a variety of techniques have been devised here for the detection of hydrazine over other comparable ions and neutral amines.

1. Introduction

Hydrazine is a chemical compound that contains two nitrogen atoms joined by a single covalent bond with the formula N_2H_4. It is a clear, colorless liquid with a smell that is similar to ammonia. It is highly reactive, volatile and flammable. Hydrazine is an essential chemical reagent employed as a strong reducing agent and very reactive base and is employed in several chemical industries as a crucial reactant in the preparation of pharmaceuticals (3-amino-1,2,4-triazole, isoniazid, and maleic hydrazide), photography chemicals, emulsifiers, textile dyes, insecticide and pesticides.[1,2] Hydrazine is frequently used as a high-energy fuel in missiles, satellites as well as in spacecraft and rocket–propulsion systems because of its highly flammable nature and high enthalpy of combustion.[3–5] Moreover, in industry, it is also used as a chemical blowing agent and metal corrosion inhibitor for boilers, preservative in nuclear and electrical power plants and antioxidant agent.[6,7] In addition, it is found that certain yeasts and some nitrogen fixing bacteria e.g. *Brocadia anammoxidans* have the ability to produce hydrazine as a by-product of natural biochemical reactions.[8] People who work in these locations for a long time are therefore under threat of poisoning by this liquid. However, its high toxicity and volatility raise safety concerns for its use. In spite of its extensive uses in industry, hydrazine is normally recognized as a convulsant, neurotoxicants, local irritants, hepatotoxins and carcinogens and therefore its adverse effect can cause environmental contamination and severe health effects on human body during its manufacture, utilization, transportation and discarding processes.[9,10] Hydrazine vapor and its aqueous solution, can be readily absorbed by oral and dermal routes or via direct breathing, causing harsh damage to kidney, liver, lungs and central parts of the nervous system along with irritation of respiratory system, dizziness, momentary blindness, blood abnormalities, nausea, coma pulmonary edema and damage of DNA in humans.[11–13] Therefore, U.S. Environmental Protection Agency (EPA) has categorized hydrazine as a prospective human carcinogen with tolerable threshold limit value (TLV) of 10 ppb.[14] Furthermore, in the past, hydrazine was applied experimentally as a therapeutic agent for the cure of sickle cell anemia, tuberculosis, and non-specific chronic illnesses.[15,16] The huge number of physiological functions in which N_2H_4 is involved requires the development of simple methods for its sensitive and selective detection. Up to now, several conventional analytical techniques, including electrochemical methods (such as coulometry,[17] capillary electrophoresis,[18] ion-selective electrode,[19] potentiometry[20] and amperometry[21]), chromatographic methods (such as HPLC,[22] gas chromatography,[23] and ion chromatography[24]), and titrimetry,[25] have been exploited for both qualitative and quantitative estimation of hydrazine. However, most of these methods generally require costly equipment, skilled operators, time consuming and complicated sample preparation which makes them impractical for real-time and on-site analysis. Again, spectrophotometry using colored derivatives, such as chlorosalicylaldehyde,[26] and p-dimethylaminobenzaldehyde[27] is also employed to sense hydrazine. Consequently, cell imaging studies (in vitro/in vivo) for hydrazine are also not

[a] *Dr. S. K. Manna*
Department of Chemistry,
Haldia Government College,
Debhog, Purba Medinipur -721657, West Bengal, India.
[b] *A. Gangopadhyay, Dr. K. Maiti, Dr. S. Mondal, Prof. A. K. Mahapatra*
Department of Chemistry,
Indian Institute of Engineering Science and Technology,
Shibpur, Howrah-711103, West Bengal, India.
E-mail: akmahapatra@rediffmail.com

possible with these methods owing to their investigation process and demolition of tissues and cell contents. Compared with these analytical approaches, the colorimetric and/or fluorescent techniques belonging to spectral field are more suitable, competent and attractive for the detection of hydrazine on account of their high sensitivity, low cost, simplicity, dependability, speediness, real-time detection and mainly turn-on fluorescent probes, which not only have easy implementation, high sensitivity and selectivity, but also have a high signal-to-noise ratio.[28] These sensing techniques are very much handy to monitor hydrazine in several environmental samples e.g. air, squander water and residues.[29] Additionally, detection with the chromogenic and/or fluorogenic probes constantly associates with ultraviolet or fluorescent emissions, which can be easily detected visually excluding any sophisticated instrumentation.

When designing chromogenic and fluorogenic probes (the host) for the recognition of small neutral molecules or analytes (the guest), it is crucial to utilize specific host – guest interactions or chemical reactions that accompany the changes of their spectroscopic (chromogenic, or fluorogenic emission) properties;

on the basis of such changes, the analytes can thus be determined.[30] If the specific interaction between an abiotic probe (host) and the guest is noncovalent and reversible, and the interaction can be converted measurable signals with a real-time response that can be easily detected, such as a fluorescent or color change or an electronic signal, the indicator is referred to as a chemosensor.[31–33] In a chemodosimeter functions through an irreversible chemical reaction between the host and the guest.[34–38] Chemosensors however interact through coordination. In this case the binding between host and guest and accompanying signal changes are reversible.[39–41] In fact, coordination is a reversible chemical reaction dependent upon changes in the concentration of the analytes which influences the concentrations of coordinated and free moiety. Chemodosimeters, function through a highly selective and usually irreversible chemical reaction with the target analyte. Hence. Chemodosimeters are often designed such that they will have appreciable selectivity towards a targert analyte. Using photo luminescent emission as detection signal, chemodosimeters exhibit high sensitivity. An observable signal is generated that has an accumulative effect depending on the concentration of the analyte. In addition, chemodosimeters usually show rapid response to the target analyte.

Dr. Saikat Kumar Manna is currently working as an Assistant Professor in the Department of Chemistry, Haldia Government College, Debhog, West Bengal, India. He has published more than 25 research papers in peer-reviewed international journals in the fields of molecular recognition and supramolecular chemistry. He obtained his Ph.D. degree in 2015 from Indian Institute of Engineering Science and Technology, Shibpur, Howrah.

Miss. Ankita Gangopadhyay obtained her Bachelor's degree with honours in Chemistry from the University of Calcutta in 2011 followed by her Master's degree in 2013 from Indian School of Mines. Dhanbad and is presently working towards her doctoral degree under Professor Mahapatra's supervision at Indian Institute of Engineering Science and Technology, Shibpur, Howrah. She has co-authored 6 papers in international peer reviewed journals so far and her focus is on both hazardous as well as biologically relevant analytes.

Dr. Kalipada Maiti obtained his M.Sc. degree in 2011 and Ph. D degree in 2016 from Indian Institute of Engineering Science and Technology, Shibpur. He is now working as a postdoctoral fellow in the Department of Chemistry, University of Calcutta.

Dr. Sanchita Mondal obtained her M.Sc. degree in 2012 from University of Calcutta, and Ph.D degree in 2017 from Indian Institute of Engineering Science and Technology, Shibpur. She is now working as a postdoctoral fellow in the Department of Chemistry, Jadavpur University.

Prof. Ajit Kumar Mahapatra, currently serves as Head of the Department of Chemistry at Indian Institute of Engineering Science and Technology, Shibpur, Howrah. He obtained his Ph.D. degree in 2001 from Bengal Engineering and Science University, Shibpur, Howrah. He has published more than 100 research papers in peer-reviewed international journals in the fields of synthetic organic chemistry, molecular recognition and supramolecular chemistry. His publications have garnered ~ 1500 citations so far. His current research activity includes fluorescent chemosensing of a diverse range of analytes such as NO, H_2S, DCP, phosgene, formaldehyde and hypochlorite to name a few.

Because of their rapid response, high sensitivity, and excellent selectivity, the design, synthesis, and application of chemodosimeters in luminescence bioimaging has attracted increasing attention and become a very active research field. Typically, chemodosimetric probes are comprised of three different moieties: (1) the reaction site, where the host responsible for the selective reaction with analyte; (2) spectroscopic or signaling moiety, whose properties should be changed upon reaction with the analyte of interest and (3) a suitable spacer or linker that connects the analyte reaction site and fluorophore moiety (sometimes the two moieties are integrated without any linker).

In this review, we will focus on the recent progress in chemodosimeters for hydrazine sensing in a systematic and comprehensive manner. Many fluorescent probes for N_2H_4 detection have been developed. All these probes use one of the following mechanisms: (1) cleavage of the acetoxy (CH_3COO–) group; (2) the nucleophilic addition-elimination on keto ester; (3) the nucleophilic substitution-elimination to tandem cyclization on halo-ester; (4) the nucleophilic addition reaction to phthalimide derivative to phthalhydrazide; (5) the chemical displacement of active methylene compound to hydrazone derivative and (6) Others different approaches.

1.1. Cleavage of the acetoxy (CH_3COO–) group

The reactive probes can be categorized by the type of chemical reactions implemented: nucleophilic additions-eliminations and substitutions as well as tandem reactions involving them. Inherently, the nucleophilic addition-elimination or substitution reactions can be used for sensing neutral or anionic analytes that are nucleophilic. For analytes having sufficient nucleophilicity nucleophilic addition-elimination or substitution reactions may be employed for sensing purposes. The addition of nucleophiles to electrophilic centers such as carbonyl carbons is categorized as the nucleophilic addition reaction and then elimination occurs when leaving group attached with the carbonyl carbon. Nucleophiles have lone pair electrons, and like Lewis bases they can donate electron pairs to electrophilic centers. Therefore, neutral or anionic analytes such as amines, thiols and cyanide etc that have lone pair electrons can act as nucleophiles. Nature of the addition products, called adducts, depend on both the nucleophiles and electrophiles.

An addition-elimination of hydrazine to ester functionality to form the corresponding acetylhydrazine or hydrazinolysis product has been widely used for the development of fluorescent probes for hydrazine analyte (Scheme 1). This

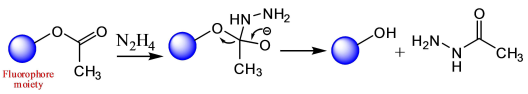

Scheme 1. Design strategy of chemodosimetric fluorescent probes for selective detection of hydrazine based on cleavage of the acetoxy group.

addition-elimination property has been extensively used for the design of various fluorescent probes for amines and thiols.[42] In this section, we focus on selected examples classified by the reaction types used for turn-on fluorescence sensing of nucleophilic neutral species like hydrazine.

Duan et al.[43] extended this concept for the development of a 4-hydroxy-napthalimide-based chemodosimeter (1) that serves as a naked eye sensor for hydrazine in DMSO: PBS buffer (1:1, v/v/pH 7.4, 10 mM) solution. Addition of hydrazine to the organo aqueous solution of probe 1 causes a decrease in the absorption peak at 343 nm and an accompanying increase in peak at 459 nm with a clearly isosbestic point at 379 nm, causing a color change from colorless to yellow. In addition, the intensity of emission band of 1 at 432 decreases gradually and a new red shifted band appears at 543 nm in presence of hydrazine. The reaction was completed immediately after the addition of hydrazine within 5 minutes, and hence, 1 could be used in real-time determination of hydrazine in environmental and biological conditions. The main reason behind changes in the optical behavior of probe is due to the deprotection of the acetate group by hydrazine and was confirmed by HPLC and HRMS analysis (Figure 1). The detection limit (LOD) was

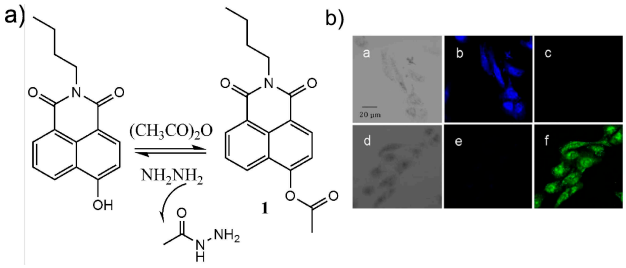

Figure 1. a) Structure of probe **1** and cleavage of acetoxy group of 1 by N_2H_4. b) Fluorescence images of 7860 cells incubated with probe 1 before (a–c) and after (d–f) treatment with hydrazine. Reprinted from Ref.,[43] Copyright (2015), with permission from Elsevier.

measured to be 0.67 ppb which is lower that of TLV (10ppb) according to EPA. Others structurally analogous primary amine and biologically important ions did not show such type of fluorescence as well as absorbance enhancement. Furthermore, the probe can be used to monitor hydrazine in live cells by fluorescence imaging and also to detect hydrazine in real water samples.

In 2016, Wu et al. synthesized an ICT-based ratiometric fluorescence turn-on probe **2** for selective detection of hydrazine (Figure 2) [44]. Probe **2** displayed an emission peak at 445 nm. However, upon addition of hydrazine, probe **2** exhibited a 100 nm red shifted emission (λ_{em} = 545 nm) as a result of switching on ICT. The fluorescence intensity ratios (I_{545}/I_{445}) demonstrated a good linear relationship with hydrazine concentrations ranging from 0–0.1 μM and detection limit of 9.40 ± 0.12 nM was determined. Probe **2** was employed to monitor hydrazine in real water samples. The authors further demonstrated that this probe is able to detect gaseous

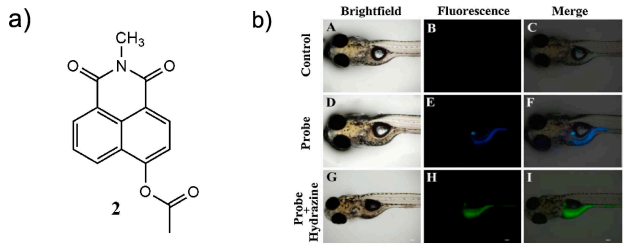

Figure 2. a) Structure of probe **2**. b) Fluorescence microscopic images of zebrafish larvae. (A–C) the control; (D–F) treated with probe **2** only and (G–I) after incubation with **2** and hydrazine. Reprinted from Ref.,[44] Copyright (2016), with permission from Elsevier.

hydrazine. Furthermore, the probe could be used to visualize hydrazine in live zebrafish.

Chang et al.[45] developed the reaction-based fluorescent turn-on probes **3–6** for hydrazine based on the dichlorofluorescein and resorufin acetates and chloroacetates (Figure 3).

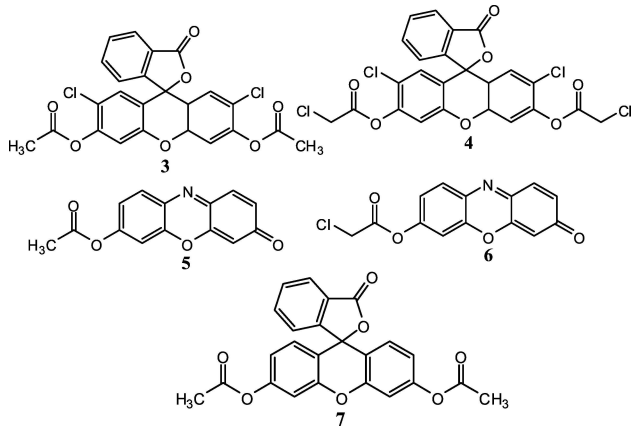

Figure 3. Structures of probes **3–7**.

These sensors displayed sensitive and selective responses toward hydrazine, accompanied by unique colorimetric and turn-on fluorescent changes. Signaling was affected by hydrazinolysis of the phenol acetate and chlorocetate moieties to their phenolic analogue. Addition of hydrazine to probe **3** and probe **5** changed the solution color to greenish yellow and pink, along with the fluorescent color changing to high green and pink respectively. These sensors showed high sensitivity and selectivity toward hydrazine with detection limits of 9.0×10^{-8} M for 2′,7′-dichlorofluorescein (**3**) and 8.2×10^{-7} M for resorufin (**5**), respectively.

Also using the fluorescein compound, Di et al.[46] synthesized another hydrazine probe **7** which shows a remarkable fluorescence enhancement in presence of hydrazine in aqueous media at neutral pH with high selectivity over other competing ions, and structurally analogous compound (Figure 3). In aqueous solution, sensor **7** was found to exhibit a very weak emission and absorption band over 490 nm owing to the closed nonfluorescent colorless spirolactam-ring form of fluorescein. Addition of hydrazine to the aqueous solution of probe displayed a prominent absorption band at 490 nm and a remarkable fluorescence enhancement at 515 nm. This observed fluorescence enhancement owing to the ring opening reaction of fluorescein followed by hydrazinolysis of phenyl acetate moiety of probe **7**. Moreover, the titration solution exhibited an obvious and characteristic color and fluorescence change from colorless to green as well as non-fluorescent to strong green fluorescent suggesting that sensor **7** can serve as a "naked-eye" indicator for hydrazine. The probe **7** showed excellent hydrazine selectivity with a detection limit down to the 30 nM range. This selectivity and sensitivity of fluorescence emission was inclusively observed in four real samples: distilled water, tap water, isoniazid and plasma. Again, Di's group prepared a **7**-coated organic membrane that can be utilized to roughly and quantitatively detect and estimate the concentration of hydrazine.

The new coumarin based chromogenic and fluorogenic probe **8** for the detection of hydrazine was developed by Yu's group[47] (Figure 4). Probe **8**, which displays initially modest

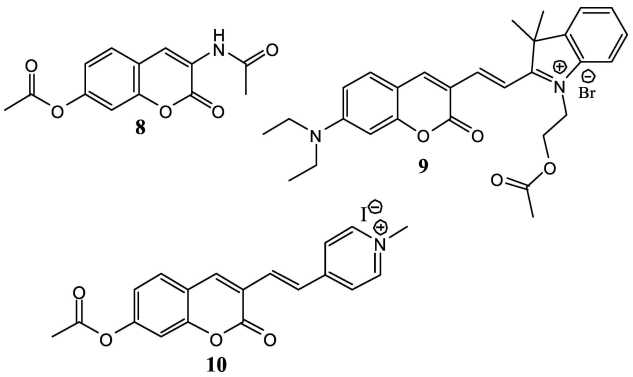

Figure 4. Structures of probes **8–10**.

fluorescence emission at 391 nm, was observed to exhibit a high sensitivity and selectivity for hydrazine. Upon gradual addition of hydrazine to the organo aqueous (10% DMSO) solution of **8** induced a red shift from 391 to 421 nm along with 2.1-fold fluorescence enhancement and a color change from colorless to bright blue. This fluorescent enhancement was mainly due to the cleavage of acetate group by hydrazine. Other competitive anions and primary amines did not show any considerable influence on the fluorescence emission of **8**.

Another coumarin-based derivative **9** was designed as probe for hydrazine in DMSO-H_2O (2: 8, v/v, 40 mM Britton–Robinson buffer solution, pH = 7) (Figure 4).[48] Probe **9** showed fluorescence enhancements (λ_{max} = 500 nm) and UV-Vis spectral changes, and which were attributed to the deacetylation of probe **9** in presence of hydrazine, accompanied by a color change from deep blue to pale yellow. The authors suggested that rate of deacetylation of probe **9** could be enhanced by increasing temperature. The authors performed a kinetic study

of the reactions of **9** with hydrazine and it was found that the reaction rate was completed within 90 min at 50 °C. Various transition metal ions except Ni(II), Pb(II) and Hg(II) and common amino compounds induced no changes in the fluorescence emission properties under the same conditions.

The fluorescence probe **10**, based on coumarin moiety, was designed and used for the detection of hydrazine by Yu et al.[49] (Figure 4). It exhibited a sensitive and selective fluorescence enhancement in the presence of biothiols, which was not observed for other representative anions (SO_4^{2-}, CH_3COO-, CO_3^{2-}, NO_2^-, SO_3^{2-}, Br^-, I^- and Cl^-), ions (Mn^{2+}, Zn^{2+}, K^+, Na^+, Co^{2+}, Ni^{2+} and Cu^{2+}) and common amines (urea, ethylenediamine, glycine, thiourea, ammonia and triethylamine. The sensing mechanism was confirmed by ESI mass spectroscopy. Confocal microscopy experiments demonstrated that **10** could be used to detect exogenous hydrazine in mitochondria.

Peng et al.[50] reported cyanine dye based NIR fluorescent hydrazine probe **11** (Figure 5). In this case, hydrazine can

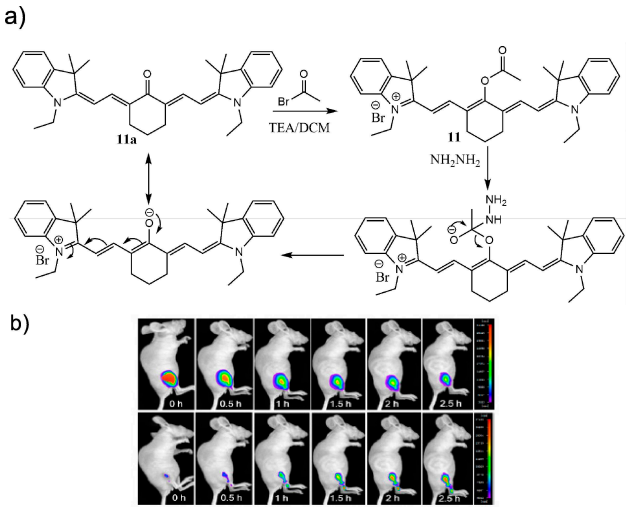

Figure 5. a) Structure and Schematic diagram of the reaction of probe **11** towards hydrazine. b) Representative fluorescence images of a nude mouse (pseudocolor) given a skin-pop injection of **11** and a consequent skin-pop injection injected with N_2H_4. Images were taken after incubation for 0, 0.5, 1, 1.5, 2, and 2.5 h, correspondingly. Reprinted with permission from Ref.[50] Copyright (2013) American Chemical Society.

selectively react with the carbonyl carbon of the acetate ester and yield a tetrahedral intermediate. This corresponding intermediate can next undergo an elimination to release the hydrazinolysized product i.e. enol form of **11a** moieties which further undergo tautomerism to give its analogous keto form, resulting in large ratiometric fluorescence response with a detection limit of 0.81 ppb in aqueous solution. Moreover, the sensor was successfully applied to detect hydrazine in real water samples quantitatively, image hydrazine in living cells in a ratiometric manner, and, for the first time, visualize hydrazine in living mice by monitoring the signal changes of two different fluorescence channels.

Recently, Zhang et al.[51] devised another NIR fluorescent probe **12** for selective and sensitive detection of hydrazine that operates based on deprotection of the acetyl group of probe **12** by reaction with hydrazine. In probe **12**, an acetyl group provides as the hydrazine specific trigger moiety and removal of acetyl group in probe **12** by hydrazine, leading to the generation of the corresponding cyanine fluorophore moiety (**12**-OH), accompanied by the large fluorescence enhancement centred at 706 nm (Figure 6). This sensing mechanism is proved

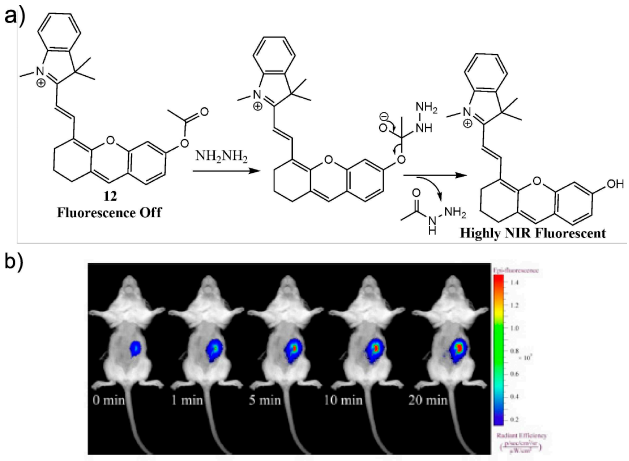

Figure 6. a) Reaction of chemodosimeter **12** with hydrazine to discharge the NIR fluorescent products. b) Representative fluorescence images of a Kunming mouse (pseudo color) given a skin-pop injection of **12** and then injected with hydrazine. Images were taken after incubation for 0, 1, 5, 10, and 20 min, respectively. Reprinted with permission from Ref.[51] Copyright (2015) American Chemical Society.

through HPLC analysis, mass spectra and theoretical study. The detection limit for hydrazine was calculated to be 5.4 ppb as fluorescence sensor and 6.1 ppb as UV sensor. Probe **12** was used to detect hydrazine in various water samples and diluted human serum samples. In addition, probe **12** was able to monitor N_2H_4 in live mouse and, for the first time, in tissues such as the liver, lung, kidney, heart, and spleen.

Recently, by incorporating a O-acetyl moiety into an dicyanomethylene-4H-pyran skeleton, Peng et al.[52] developed the NIR fluorescent chemodosimeter **13** which displayed an off-on fluorescent response toward hydrazine (Figure 7).The probe **13** has a detection limit as low as 5.7×10^{-8} M and a little response time of 1 min. The probe affords a two-photon cross-section d_{max} as high as 30 GM at 830 nm in solution (Ethanol/PBS = 5/5, pH = 7.4) and has been effectively applied to detect N_2H_4 in living cells by two-photon microscopy imaging. Moreover, filter paper coated with the probe **13** could be used to detect hydrazine in solution.

A 2-thiophenecarbonyl moiety derived hemicyanine skeleton (**14**) has been synthesized by Wang et al.[53] as a NIR fluorescent probe for hydrazine (Figure 8). Very low detection limit of the probe (0.78 ppb) allow the monitor and image hydrazine in living cells, tissues and mice. This is for the first time where hydrazine could be detected in deep living tissue.

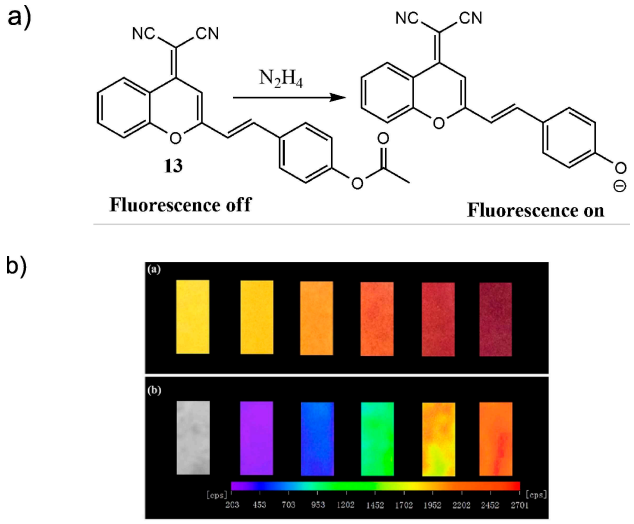

Figure 7. a) Reactions of **13** with hydrazine at pH 7.4. b) (a) The UV color and (b) fluorescence intensity changes of the pre-strained filter paper with probe **13** in presence of different concentrations of hydrazine. Reprinted from Ref.,[52] Copyright (2017), with permission from Elsevier.

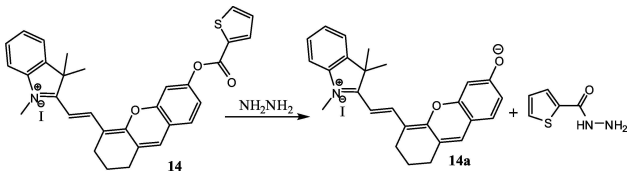

Figure 8. Reaction of chemodosimeter **14** with hydrazine to release the NIR fluorescent products (**14a**).

Mahapatra's[54] laboratory developed two colorimetric and turn-on fluorescent probes **15** and **16** for hydrazine based on addition elimination reaction (Figure 9). Using UV-vis spectroscopy, fluorescence spectroscopy, kinetic studies and ^{1}H NMR titrations, along with theoretical studies, probes **15** and **16** was reported to be the highly selective for hydrazine, with limit of detection of 0.55 and 4.5 μM in aqueous DMSO (1:2, v/v) HEPES buffer (pH = 7.4) solution. Compound **15** could also be exploited for the bioimaging of hydrazine in vero cells.

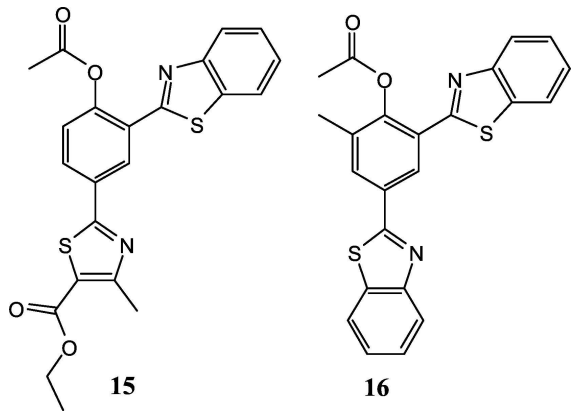

Figure 9. Structures of hydrazine probes **15** and **16**.

Zhan et al.[55] reported a ratiometric fluorescent probe **17** for the detection of hydrazine based on a FRET signaling mechanism (Figure 10). Before reaction with hydrazine, probe **17** showed a characteristics emission peak of coumarin at 474 nm. However, a fluorescence increase at 533 nm and a decrease at 474 nm were found in the presence of hydrazine due to the ring open reaction of fluorescein moiety. Again, this fluorescence changes is associated with color change from blue to strong green fluorescence with a detection limit of 0.0474 μM. This probe was effectively applied to dual-channel imaging of hydrazine in living cells.

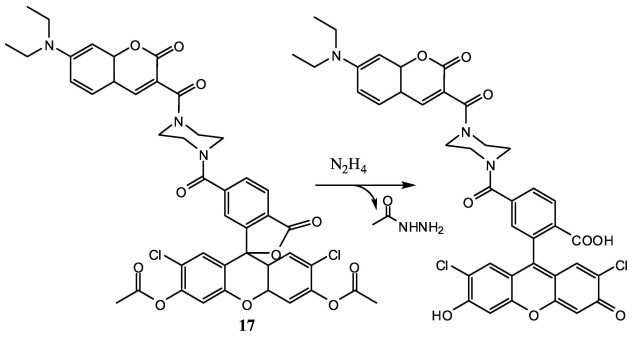

Figure 10. Reaction of **17** with hydrazine at pH 7.4.

Chen et al.[56] designed two ESIPT based probes **18** and **19** for micromolar detection of hydrazine in solution as well as in live samples (Figure 11). These probes display excellent

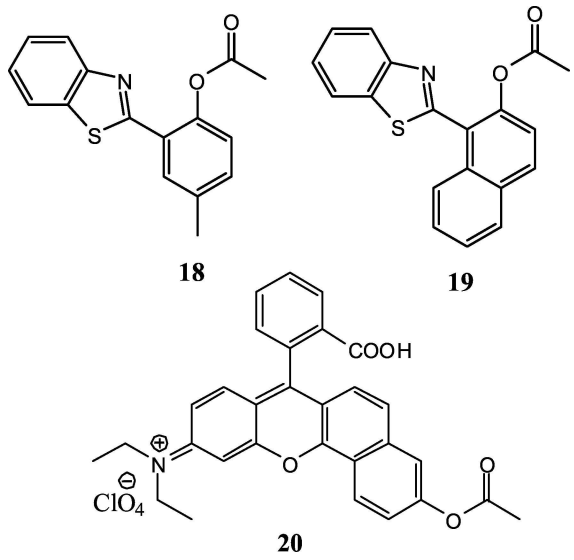

Figure 11. Structures of hydrazine probes **18–20**.

selectivity for hydrazine over other comparatives chemical species such as such as S^{2-}, Cl^-, Br^-, I^-, ClO_4^-, CO_3^{2-}, H_2O_2, ClO^-, HPO_4^{2-}, HSO_3^-, NO_3^-, t-BuOOH, $ONOO^-$, SCN^-, SO_4^{2-}, NO_2^- and ROO^-. Moreover, these probes could be used for the vapor phase detection of hydrazine using the handy test-kit.

The same strategy was utilized by Lin's group[57] to design hydrazine selective probe **20** which was used for imaging mitochondrial N_2H_4 in living cells and imaging N_2H_4 in living tissues and mice (Figure 11). Probe **20** showed high sensitivity towards hydrazine, with a detection limit of 3.65×10^{-7} M in Britton-Robinson buffer (5% ethanol, pH = 7.4) solution.

Now, acetoxy is utilized for the protection of alcoholic –OH groups during selective chemical transformations. Deprotection is achieved under highly acidic or basic conditions. Hence, sensing protocols for hydrazine involving the acetoxy group tend to be pH sensitive. On the other hand, cleavage by hydrazine yields acetic acid as a by-product which being a considerably weak organic acid does not carry the potential of significant impact on cell viability. This makes the acetoxy group an attractive choice for probes targeted towards investigation of intracellular hydrazine concentrations at physiological pH.

1.2. The nucleophilic addition-elimination on keto ester

Several chemodosimetric probes for hydrazine based on "protection-deprotection" sequence was reported here. In presence of hydrazine, ester protected (levulinate group) probes becomes deprotected through an extensive addition-condensation–cyclization–elimination sequence, leading to changes in its photophysical properties. As a result, generated deprotected probes showed its characteristics colorimetric and fluorometric signaling behaviors.[58] The sensing mechanism is that the probe **A**, first reacts with hydrazine to form **I**, which subsequently undergoes cleavage of the ester function to form amide ring and the product **P** (Scheme 2).

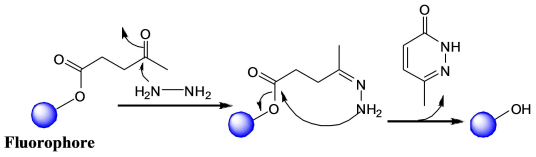

Scheme 2. Design strategy of chemodosimetric fluorescent probes for selective detection of hydrazine based on nucleophilic addition-elimination on keto ester.

Chromone derivative (**21**) was used by Ju et al.[59] in a protection–deprotection approach for the selective detection of hydrazine in DMSO–H_2O (5:1, v/v) solution. Probe **21** showed very weak emission peak at 410 nm because of the presence of oxopentanoyl group which blocks the ESIPT mechanism. But in the presence of hydrazine, probe **21** undergoes deprotection to form **21 a**, thereby enabling ESIPT and shifting the weak fluorescence emission to large fluorescence emission at 408 nm (~2-folds) and 535 nm (~60-folds) respectively (Figure 12). The detection limit of this hydrazine selective probe was deter-

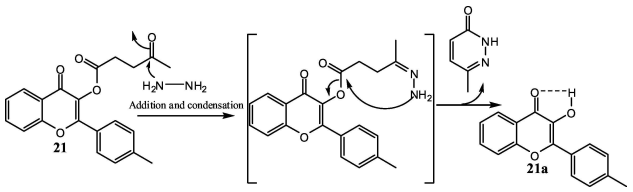

Figure 12. The reaction of probe **21** with hydrazine for the selective detection of hydrazine.

mined to be 0.016 μM (0.512 ppb), which is below the safety level (10 ppb) as recommended by EPA. Lastly, the results of fluorescence imaging experiments reveal that this probe can be employed to image hydrazine in Eca-109 cells.

Utilizing this type of approach, Chang et al.[60] also developed a new levulinate coumarin derivative, **22**, for selective detection of hydrazine (Figure 13). At pH 4.5, **22**

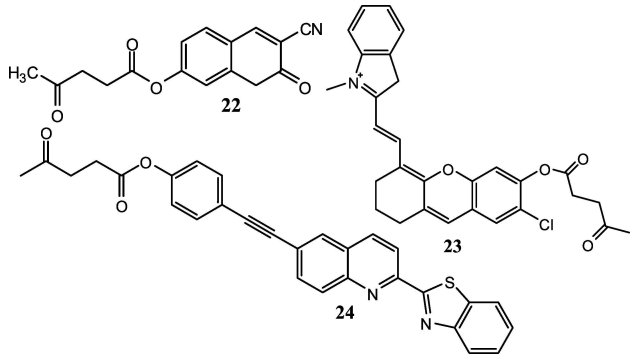

Figure 13. Structures of hydrazine probes **22–24**.

exhibits UV-Vis absorption band at 307 nm and 336 nm, shifted towards absorption band centred at 426 nm in presence of hydrazine. The probes have high selectivity for hydrazine and display fast colorimetric responses involving changes from colorless to greenish yellow. The probe **22** shows weak emission at 458 nm in 30% aqueous DMSO solution at pH 4.5. Titration of **22** with hydrazine results in the enhancement (up to 250-fold) of fluorescence intensity at 458 nm and colorless to deep blue emission takes place. Upon addition of different anionic and cationic species **22** does not show such type of development of new band in absorption as well as in emission behavior. The detection limit was found to be 0.08 ppm, indicating that the probe **22** was highly sensitive towards hydrazine.

In 2013, Lin's group[61] developed the NIR fluorescent turn-on probe **23** to selectively detect hydrazine in blood serum and live cells on the basis of the deprotection of levulinate group (Figure 13). The probe displayed very weak fluorescence at 725 nm when the hydroxyl group was alkylated, but was

converted into the highly fluorescent deprotected product with **23**-fold enhancement in the presence of hydrazine. The probe (**23**) has been shown to detect hydrazine up to 2.3 ppb at pH 7.4 which is lower than EPA threshold (10ppb). Furthermore, the probe can be used to image hydrazine in living cells.

Meng et al.[62] reported the selective and sensitive detection of hydrazine in a HEPES/THF (1:9, v/v,) solution with a ratiometric two-photon fluorescent probe **24** based on quinoline derivative (Figure 13). It has been revealed that probe **24** demonstrates a high selectivity for hydrazine than other competitive amines. This probe was effectively applied for monitoring hydrazine in living CHO cells under two-photon excitation with a ratiometric signal at low cytotoxicity. Furthermore, the probe **24** coated filter papers were also used for the vapor phase detection of hydrazine.

Recently, BODIPY-based sensor **25**, bearing pyrene butyrate-linked moiety, was developed for the selective and sensitive detection of hydrazine by Mahapatra et al..[63] Upon gradual addition of hydrazine to the H_2O–DMSO (3: 7, v/v, 10 mM HEPES buffer, pH 7.4) solution of probe **25**, the fluorescence intensity bands at 456 and 516 nm penetratingly decreases along with the emission color change from bright green to colorless under a UV lamp, allowing "naked-eye" detection of hydrazine. Probe **25** selectively reacted with hydrazine to form compound **25a** and **25b** and showed turn-off fluorescence, probably due to the selective deprotection of the 4-oxo-4-pyrenylbutyrate of probe **25** by hydrazine and generate **25a** (Figure 14). The reaction between probe **25** and

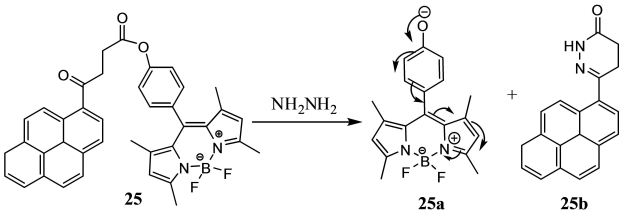

Figure 14. Reactions of **25** with hydrazine at pH 7.4.

hydrazine was monitored by ^{1}H NMR and mass spectral analysis. Moreover, probe **25** was successfully employed for vapor phase detection of hydrazine and this probe was also used for imaging hydrazine in living cells.

Ketones being very good hydrogen bond acceptors, attempts at sensing hydrazine through probes of this category in highly polar media may lead to mixed results including possble interference from weaker nucleophiles than hydrazine due to diminished electrophilicity of the keto carbon induced by hydrogen bonding. On the other hand, ketones are robust when it comes to reactivity in presence of both acids and bases which leaves room for sensing applications over wide pH ranges.

1.3. Nucleophilic substitution-elimination to tandem cyclization on halo-ester

Another protection-deprotection strategy was reported here for the selective detection of hydrazine. Nucleophilic substitution followed by cyclization and elimination has been used for the development of chemodosimeters for hydrazine (Scheme 3).

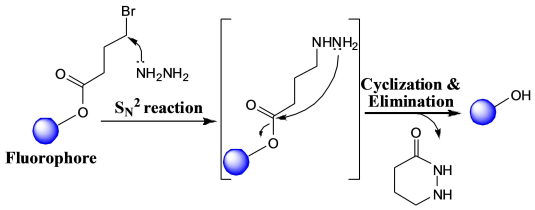

Scheme 3. Design strategy of chemodosimetric fluorescent probes for selective detection of hydrazine based on nucleophilic substitution reaction followed by cyclization and elimination.

Goswami and co-workers[64] designed chemodosimeter **26**, containing bromo-ester group that selectively reacts with hydrazine through considerable substitution-cyclization-elimination sequence to give deprotected fluorescent moiety (Figure 15). Generally, probe **26** was non-fluorescent in aqueous

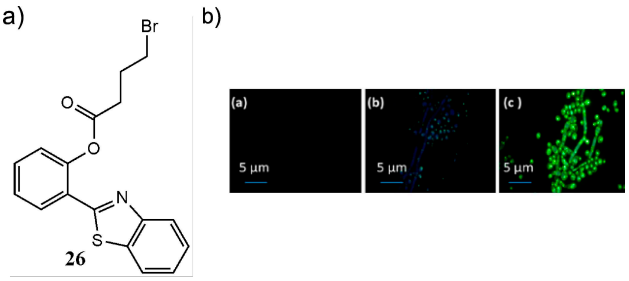

Figure 15. a) Structure of hydrazine probe **26**. b) Fluorescence microscope images of (a) Candida albicans cells, (b) cells treated with probe **26**, (c) cells treated with probe **26** + N_2H_4. Scale bar: 5 μm. Reprinted with permission from Ref.[64] Copyright (2013) American Chemical Society.

organic solvent but in presence of hydrazine induced a fluorescence turn on response. Probe **26** showed an emission band at 368 nm and upon gradual addition of hydrazine causes a large red shift of the fluorescence maximum of about 90 nm from 368 to 458 nm. The fluorescence intensity at 368 nm was gradually decreased, whereas the intensity at 458 nm gradually increased and saturated after 1 equiv. of hydrazine was added. The ratio of emission intensities at 368 and 458 nm (I_{458}nm/I_{368}nm) increased linearly with the hydrazine concentration from 1 to 9.5 μM. Chemodosimeter **26** responded quickly to hydrazine, and the first order rate constant was calculated to be $k = 8.1 \times 10^{-3}$ s^{-1} and the detection limit was calculated 2.2 ppb which was much lower than that of TLV (10ppb)

recommended by EPA and WHO. Moreover, an easy-to-prepare, short-response-time test kit was prepared by simply dipping TLC plate into a solution of a probe **26** for the naked eye detection of hydrazine. The probe **26** was further used to detect intracellular hydrazine in live cells.

In 2014, this group[65] reported another colorimetric and fluorescent chemodosimeter **27** for the selective detection of hydrazine based on substitution-cyclization-elimination approach (Figure 16). Probe **27** displayed an absorption peak at

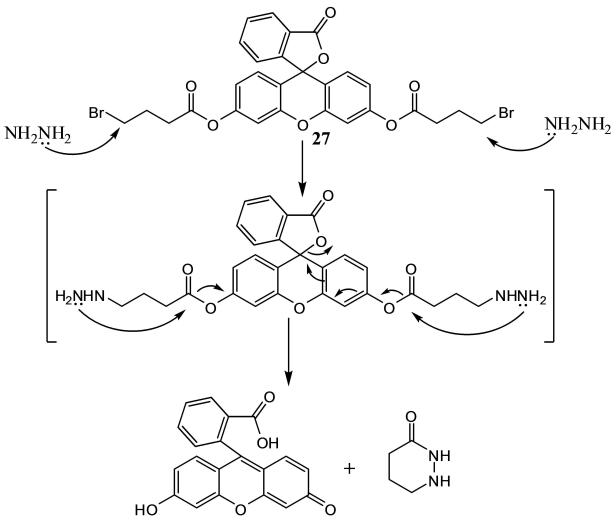

Figure 16. Reaction mechanism of probe **27** with hydrazine.

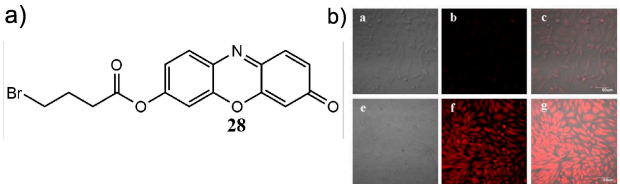

Figure 17. a) Structure of hydrazine probe **28**. b) Confocal microscopic images of Chinese hamster ovary (CHO) cells incubated with probe **28** before (a–c) and after (e–g) treatment with hydrazine. (a & e) Bright-field images; (b & f) red channel; (c & g) Merged images. $\lambda_{ex} = 543$ nm, scare bar = 50 mm. Reprinted from Ref.,[66] Copyright (2014), with permission from Elsevier.

of phosphate buffer saline (PBS, pH 7.0, 20 mM) and DMSO (1:9, v/v) solution. This probe could detect hydrazine in solution at very low concentration (4.8 ppb) by reaction to form the corresponding 3-hydroxyflavone (**29a**), thereby allowing ESIPT process and generating a strong green emission with 55-fold enhancement (Figure 18). The probe was capable of imaging hydrazine in living HeLa cells.

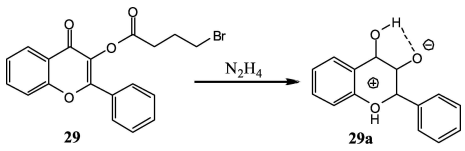

Figure 18. Reactions of **29** with hydrazine at pH 7.4.

496 nm with 27 folds enhancement in presence of hydrazine, which causes color changes from colorless to greenish-yellow. Free probe **27** was itself not fluorescent (Quantum yield = 0.01) but the addition of 4 equiv. hydrazine led to the strong emission at 516 nm (Quantum yield = 0.54) with appearance of strong green color fluorescence. However, other cations, anions, and neutral bases [Cd^{2+}, Ag^{+}, Pd^{2+}, Ni^{2+}, Zn^{2+}, Cu^{2+}, Mn^{2+}, Mg^{2+}, Fe^{3+}, Co^{2+}, Cr^{3+}, Hg^{2+}, F^{-}, NO_3^{-}, OCl^{-}, HSO_4^{2-}, HSO_3^{-}, SO_3^{2-}, SO_4^{2-}, $NH_2(CH_2)_2NH_2$, NH_3 and NH_2OH] did not cause any noteworthy changes in the absorption and emission of probe **27**. Based on the apparent color change, the probe **27** can be used for the visual detection of hydrazine and its detection limit was found to be 3.881×10^{-8} M.

Zhu et al.[66] described another bromo-ester group containing non-fluorescent probe **28** for the selective detection of hydrazine (Figure 17). Addition of increasing concentrations of hydrazine to the aqueous acetonitrile solution of **28** results in a remarkable color change from colorless to red along with the appearance of strong fluorescence emission at 584 nm. It was observed that the sensing behavior of receptor **28** toward hydrazine was not affected in presence of other metal cations and anions. The probe was also used to detect hydrazine in live CHO (Chinese hamster ovary) cells using confocal microscopy.

Zhu et al.[67] designed the sensitive and selective fluorescence turn-on probe **29** to detect hydrazine in a mixture

In 2016, Zhu et al.[68] reported another 3-hydroxyflavone derivative **30** to detect hydrazine, which operates by a bromo ester deprotection mechanism (Figure 19). Probe **30** showed a very strong emission band at 590 nm in DMSO–PBS (9 : 1, v/v, pH = 7.3, 15 mM PBS) solution. However, on addition of hydrazine, the fluorescence intensity of the probe **30** gradually decreased. The fluorescence intensity at 590 nm was linearly proportional to hydrazine concentration (0–20 mM) and a limit of detection of 0.36 μM was determined. Various analytes such as Fe^{3+}, K^{+}, Mn^{2+}, Mg^{2+}, Zn^{2+}, Pb^{2+}, Ni^{2+}, Hg^{2+}, Co^{2+}, S^{2-}, NO_2^{-}, NO_3^{-}, HSO_4^{-}, ClO_4^{-}, $H_2PO_4^{-}$, Cl^{-}, Br^{-}, I^{-}, F^{-}, ClO^{-}, H_2O_2, t-BuOOH did not induce any obvious emission spectral changes. Moreover, sensing mechanism was confirmed by ^{1}H-NMR and mass spectroscopy. This sensor was successfully applied to detect low concentration of hydrazine in real water samples.

A 1,8-naphthalimide derivative based probe **31** was utilized by Xu et al.[69] as the efficient chemodosimeter for the detection of hydrazine (Figure 19). In absence of hydrazine, the probe **31** showed an emission peak at 420 nm due to disruption of ICT process. However, when hydrazine is added to the HEPES buffer (10 mM, pH 7.4, 10% CH_3CN) solution of **31**, the color of the solution instantly changes from blue to yellow green, corresponding to a red-shift of the emission peak to 550 nm., as a result of switching on ICT. In addition, hydrazine can be detected quickly by employing a probe **31** containing paper

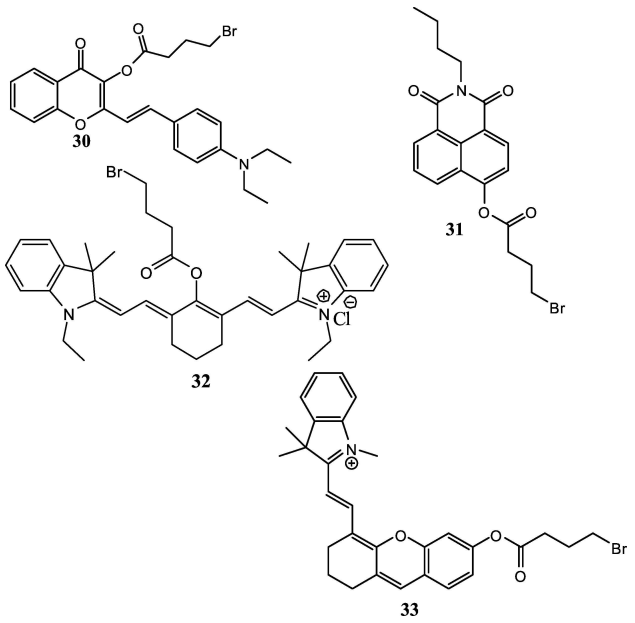

Figure 19. Structures of hydrazine probes **30–33**.

test strip system. The detection limit of **31** for hydrazine was calculated to be 0.27 μM. Cell imaging experiments showed that **31** was able to sense the intracellular hydrazine in A549 cells.

Recently, Lu and coworkers[70] devised a two-emission colorimetric NIR fluorescent probe **32** for selective detection of hydrazine that functions on the basis of substitution, cyclization and elimination reactions (Figure 19). Probe **32** showed a spiky and strong absorption band in the NIR region, at 782 nm, which disappeared in the presence of hydrazine and consequently a new band at 547 nm was formed, which resulted in a change in the color from blue-green to red that could be examined by the naked eye. Again, upon gradual addition of hydrazine, the probe **32** displayed a notable fluorescence enhancement at 627 nm compared to the decrease at 814 nm when excited at different wavelength. This probe showed a high selectivity over different comparative analytes. Probe **32** was found to have a low detection limit of 0.38 ppb for hydrazine. Moreover, cell experiments suggested that probe **32** has the ability to image hydrazine in living HeLa cells and mice with low cytotoxicity.

In recent times, Lu et al.[71] developed a NIR based fluorescent dye (**33**) for selective detection of hydrazine (Figure 19). 4-bromobutyl group connected with this probe, being leaving out upon reaction with hydrazine, leads to remarkable emission enhancement at 715 nm. There was a significant naked eye and fluorescence color change of the probe by hydrazine, preferable for its qualitative and quantitative detection. Most importantly, the probe **33** can detect hydrazine in living cells and mice.

Using a similar strategy, Qian et al.[72] synthesized fluorescent probe **34** for the detection of hydrazine by utilizing the phenomenon of excited-state intramolecular proton transfer (ESIPT) (Figure 20). Probe **34** does not have any ionizable protons and hence it was unable to participate in ESIPT

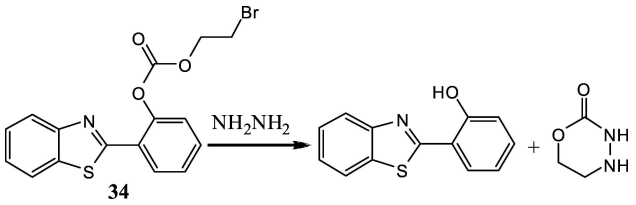

Figure 20. Reaction of probe **34** with hydrazine.

process. Therefore, probe **34** displayed a very weak fluorescence at 465 nm. In presence of hydrazine, PET is eliminated and a remarkable fluorescence enhancement (50-fold) was observed at 465 nm. The authors found that the fluorescence intensity upon reaction with hydrazine increased with time and reached a plateau at 10 min. The detection limit for hydrazine was determined to be 0.147 μM. In addition, this probe was able to sense hydrazine in HeLa cells.

Brominated esters are generally hazardous and their handling entails proper precaution. Also, the coupling reactions by which these probes are prepared often give poor yields. So, from a synthetic standpoint it leaves room for better alternatives. The electrophilicity of the carbon centre is also weak while the adjoining C–H bonds acidic. This means hydrazine could also act as a potential base in addition to its nucleophilic activity. Literature survey indicates that some fluorophores are apparently better than others at facilitating this sensing mechanism although it is not properly rationalized. With the right fluorophore, however, sensing performance is outstanding.

1.4. Nucleophilic addition reaction to phthalimide derivative to phthalhydrazide

The Gabriel amine synthesis[73,74] reaction has attracted tremendous attention in the area of chemistry and biology. This reaction involves the two step chemical conversion of primary alkyl halides to primary amines, in which potassium phthalimide is first alkylated and then the resulting N-substituted phthalimide is hydrolyzed by acid or base. However, it is found that basic condition hydrolysis step is the rate-limiting step. Therefore, this hydrolysis step has been modified by using hydrazine for the cleavage of the phthalimide under mild and neutral conditions which is known as Ing-Manske procedure.[75] In general, due to the high reaction activity, hydrazinolysis affords improved results, faster response and more sensible reaction conditions. In view of that, a mechanistic way for this reaction is shown in Scheme 4. In recent times, this chemistry was applied for the detection of hydrazine and in this section; we reported several above-mentioned reaction-based probes for hydrazine.

Xu and coworkers[76] constructed a novel fluorescent probe **35** for hydrazine based on Gabriel synthesis (Figure 21). Probe

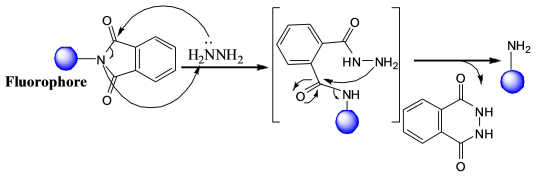

Scheme 4. Design strategy of chemodosimetric fluorescent probes for selective detection of hydrazine based on the Gabriel amine synthesis mechanism.

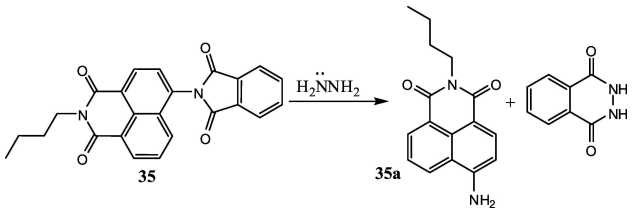

Figure 21. Reaction of probe **35** with hydrazine.

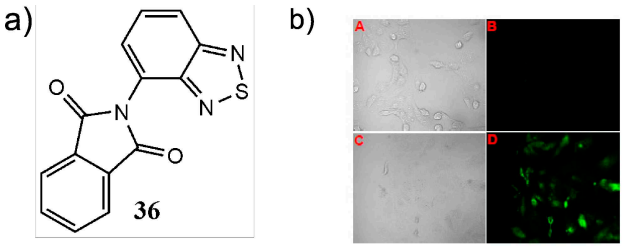

Figure 22. a) Structure of hydrazine probe **36**. b) Confocal microscopic images of Vero 76 cells (Vero 76, ATCC No CRL-1587) incubated with probe **36** before (A & B) and after (C & D) treatment with hydrazine. (A & C) Bright-field images; (B & D) Fluorescence images. Reproduced from Ref.[77] with permission of The Royal Society of Chemistry.

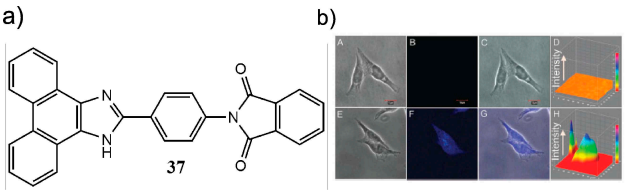

Figure 23. a) Structure of hydrazine probe **37**. b) Confocal laser scanning microscopic of Hct116 colon cancer cells incubated with probe **37** as the control: (A) bright field; (B) dark field laser; (C) overlay images of (A) and (B); and (D) 3D intensity plot of image (B). (E–H) CLSM images of Hct116 cells treated with **37** + N_2H_4: (E) bright field; (F) dark field laser; (G) overlay images of (E and F); and (H) 3D intensity plot of image (F). $\lambda_{Ext}/\lambda_{Em}$ = 352/455 nm; scale bar: 10 μm. Reproduced from Ref.[78] with permission of The Royal Society of Chemistry.

35 composed of 1, 8-napthalimide as a fluorescent probe and a phthalimide part as a reactive unit. In H_2O/DMSO (4:6, v/v) solution, hydrazine favors phthalimide deprotection with the release of electron withdrawing amino group (**35 a**) and gives a dramatic color change from colorless to yellow. Compound **35** displayed a remarkable fluorescence enhancement (100 times) at 540 nm upon reaction with hydrazine. The fluorescence intensity at 540 nm was linearly proportional to [N_2H_4] concentration in the range of 1–50 μM and the detection limit was found to be 0.3 ppb which is lower than the TLV value. However, other anions (Cl^-, Br^-, I^-, SO_4^{2-}, SO_3^{2-}, ClO_4^-, HCO_3^-, SCN^- and HPO_4^{2-}) and cations (Hg^{2+}, Co^{2+}, Cr^{3+}, Cd^{2+}, Fe^{3+}, Ni^{2+}, Zn^{2+}, Cu^{2+}, Al^{3+}, Mg^{2+}, Ca^{2+} and Ag^+) did not lead to any observable absorption and emission changes. In addition, probe **35** was able to detect hydrazine in gas phase and in living cells. For vapor phase hydrazine detection, probe loaded TLC plate was kept in hydrazine containing jar for 10 min and fluorescence color changed from colorless to yellow. The gaseous state hydrazine detection limit was 111.7 mg m^{-3}.

Mahapatra and coworkers[77] disclosed benzothiadiazole based probe **36** for the selective and sensitive detection of hydrazine based on Gabriel mechanism (Figure 22). In H_2O–DMSO (4:6, v/v, 10 mM HEPES buffer, pH 7.4) solution, only hydrazine induced turn on fluorescence responses at 498 nm, accompanied by the emission color changes from dark to bright green, which could be observed by the naked eye. The fluorescence intensities of probe **36** showed a good linear relationship with the hydrazine concentration ranging from 0.025–1.5 μM and its detection limit was found to be 2.9 ppb. Moreover, cytotoxicity and confocal scanning microscopy experiments showed that probe **36** had excellent biocompatibility and was able to image hydrazine in live Vero 76 cells.

Recently, Das et al.[78] reported a biocompatible and fluorescent chemodosimetric probe **37** for hydrazine based on phenanthroline derivative (Figure 23). The probe **37** selectively showed large fluorescence enhancement (60-fold) towards hydrazine over various amines and other cationic and anionic analytes. The fluorescence enhancement at 430 nm exhibited a linear response to 0–30 μM hydrazine with a very low detection limit of 1.5 ppb. This fluorescence enhancement was attributed to the hydrazinolysis reaction of probe **37**. In spite of high selectivity, the time-dependent fluorescence response study showed that the reaction was complete within 40 min, and the rate constant (k) was found to be 2.76×10^{-4} s^{-1}. The author developed **37** containing paper test strip system for rapid detection of hydrazine in environmental water sample. Moreover, the results of confocal microscopy experiments reveal that probe **37** can be employed to assay the in vitro enzymatic generation of N_2H_4 in Hct116 or HepG2 cells. Notably, this probe was employed as a protective reagent against toxicity induced by the tuberculosis drug isoniazid.

In order to get perfect and sensitive detection of hydrazine, the same group[79] reported a chemodosimeter **38** based on colorimetric, fluorometric and chemiluminometric output signal (Figure 24). This dosimeter molecule contains a 7-amino-4-methylcoumarin (AMC) moiety whose 7-amino group is protected by 3-amino phthalic anhydride. In presence of hydrazine, probe **38** undergoes hydrazinolysis to give deprotected compound AMC and luminol. Titration of probe **38** with hydrazine produced a new absorption peak at 360 nm (isosbestic point at 380 nm), with a simultaneous decrease of

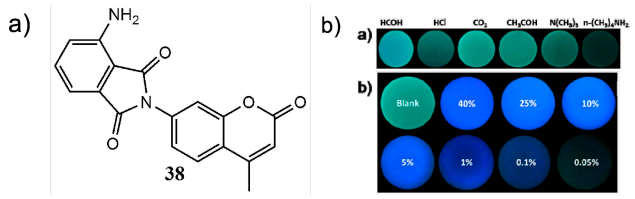

Figure 24. a) Structure of hydrazine probe **38**. b) (a) Fluorescence color changes of probe **38** coated TLC plates after exposure to several of vapor gases (formaldehyde, HCl, CO_2, acetaldehyde, trimethylamine, and n-butylamine). (b) Fluorescence color changes of **38** coated TLC plates after exposure to different concentrations of hydrazine aqueous solution. Reprinted with permission from Ref.[79] Copyright (2014) American Chemical Society.

the original maximum absorption at 410 nm. This change was associated with a visually detectable change in color from yellow to transparent. In addition, the sensor exhibited strong ratiometric emission at 420 nm with 23-fold enhancement in presence of hydrazine with limit of detection 0.1 μM. Various primary amines including hydroxyl amine, ethylene diamine, ammonia, methyl amine, urea and others cations, anions did not display any remarkable emission changes. Moreover, fluorescent hydrazine probe was suitable for the detection of hydrazine in living Hela cells. Again, the authors reported that the probe **38** could be used to detect gaseous hydrazine selectively in the environment.

Probe **39** containing the phthalimide group was used for the detection of hydrazine (Figure 25).[80] Upon addition of

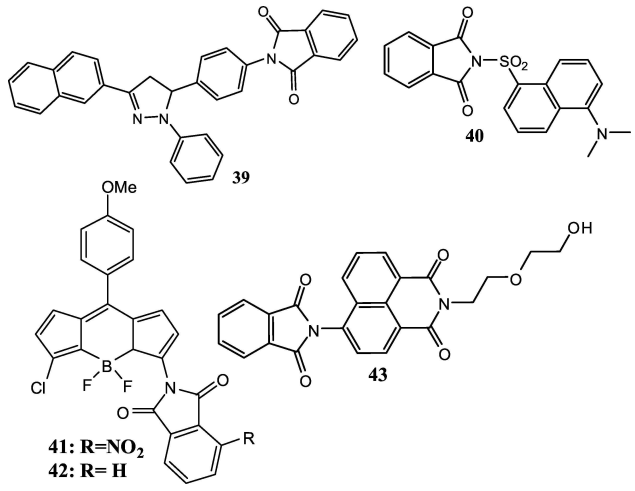

Figure 25. Structures of hydrazine probes **39–43**.

hydrazine to the solution of probe **39** in PBS buffer (10 mM, pH 7.4, 30% CH_3CN, 25 °C), the absorption peak shifted from 380 nm to 370 nm. In absence of hydrazine, effective PET takes place from the pyrazoline fluorophore to the phthalimide moiety and therefore probe **39** showed very weak emission at 450 nm. However, selective deprotection of phthalimide group by hydrazine 'turn-off' the PET process and gave rise to notable fluorescence enhancement (~84.7 folds) at 490 nm, accompanied by a color change from colorless to bright blue. It was found that other cations, anions and amines exhibits no emission changes under the experimental conditions, indicating the high selectivity of probe **39** for hydrazine over other analytes. Kinetic studies experiment was also carried out and it was found that the emission intensity upon reaction with hydrazine increased with time and reached a plateau at 4 min. The limit of detection was calculated to be 0.0622 μM (1.99 ppb). The authors also reported the vapor phase detection of hydrazine by using easily available filter paper. The probe **39** can also be used for the detection of hydrazine in living cells.

Zhao et al.[81] reported the sensitive colorimetric and fluorometric hydrazine probe **40** (Figure 25). Probe **40** displayed an absorption band at 365 nm in HEPES buffer (pH 7.0, 20 mM) and DMSO (1/9, v/v). Upon addition of hydrazine, the absorption at 365 nm decreased and was blue shifted (33 nm). The color of the solution changed from yellow to colorless. Also, in the presence of hydrazine, the emission intensity was enhanced and red-shifted from 475 to 512 nm, resulting in a color change from light yellow to strong greenish-yellow. Moreover, probe **40** has the capability of detecting hydrazine in tap water and yellow river water sample. Moreover, confocal microscopic imaging proved that the probes could be employed for detecting hydrazine in HeLa cells.

Liu et al.[82] synthesized two BODIPY based fluorescent chemodosimeters (**41 & 42**) for hydrazine detection through Gabriel reaction mechanism (Figure 25). Due to complete hydrolysis followed by release of N-protected group sensor **41** revels turn-on fluorescence response. Compound **42** undergo incomplete hydrolysis in addition of hydrazine, quenching in fluorescence occurred due to PET effect.

Using the above strategy, Lin et al.[83] designed the probe **43** that was shown to display selective and sensitive recognition toward hydrazine over other tested cations and anions (Figure 25). When hydrazine was added to the ethanolic aqueous solution [PBS buffer solutions (pH 7.2, 10 mM) in EtOH (1:9, v/v)] of probe **43**, absorption band was shifted from 344 nm to 439 nm with an obvious color changes from colorless to yellow and fluorescence emission was shifted from 467 nm to 528 nm. However, probe **43** was sensitive toward pH and was proficient to detect intracellular hydrazine in living cells.

Very recently, Li and coworkers[84] have done a classic job by putting two reactive units, phthalimide and acetyl ester group, in one fluorophoric system (**44**). Upon reaction with hydrazine a turn-on response was observed at 525 nm where the other interfering species did not show any significant change. The selective deprotection of phthalimide by hydrazine would rupture the PET process. Whereas, hydrolysis of acetyl ester and formation of free phenol hydroxyl (**44a**) restored the ICT process which is flowed by the opening of the spirolactum ring responsible for fluorescence enhancement (Figure 26). The probe **44** could be applied for detection of hydrazine from real water sample as well as in live cell.

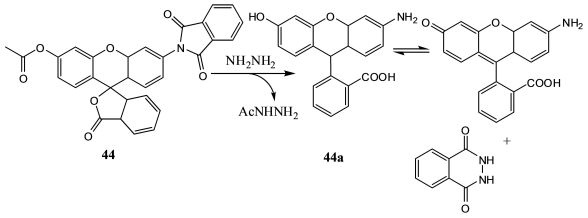

Figure 26. Reaction of probe **44** with hydrazine.

Phthalimide derivatives are excellent choices for intracellular sensing of hydrazine due to low acute toxicity. This is a tremendous advantage of this category of probes. Besides, many designs are such that a fluorophore bearing an amino functionality is generated upon chemodosimetric reaction. If a suitably electron withdrawing group is attached to the fluorescence signalling unit then the fluoroscence will be significantly red shifted upon reaction with hydrazine. Thus ratimetric sensing can be enabled. The high acidity of the imido N–H does somewhat restrict sensing in heavily basic media. But this is a minor disadvantage that is outweighed by the benefits.

1.5. Chemical displacement of active methylene compound to hydrazone derivative

In this section, the arylidenemalononitrile group has been utilized as a selective and sensitive reactive moiety for the design and development of hydrazine-based probes, in which the particular reaction between arylidenemalononitrile moiety and hydrazine yielded the product hydrazone (Scheme 5) [85].

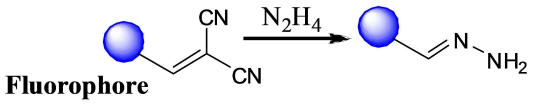

Scheme 5. Design strategy of chemodosimetric fluorescent probes for selective detection of hydrazine based on the formation of hydrazone derivative from active methylene group.

This hydrazone formation is related with the changes of UV-Vis and fluorescence emission properties of the probes.

Using this strategy, Peng et al.[86] designed and synthesized a ratiometric sensor **45** for hydrazine based on ICT mechanism from electron donor 7-diethylamino-1,4-benzoxazin-2-one (DEAB) to 3-methlenemalononitrile group (electron acceptor) (Figure 27). Addition of hydrazine to acetate buffer (pH 3.7, 10 mM)-DMSO (1/9, v/v) solution of probe **45** generated a new absorption peak at 460 nm with a concomitant decrease of the original maximum absorption at 598 nm, which was also observed by naked eye detection of a color change from purple to yellow. When excited at 510 nm, probe **45** exhibited emission at 639 nm, and with increasing concentration of hydrazine peak at 639 nm significantly decreases while a new

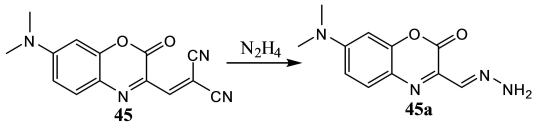

Figure 27. Reaction of probe **45** with hydrazine.

red shifted band at 564 nm was concurrently appeared, as a result of ICT process. This ratiometric behavior of probe **45** toward hydrazine was mainly due to the formation of the product **45 a**. The formation of this product (**45 a)** was monitored by IR spectra, mass spectroscopy and density functional theory (DFT) calculations. Importantly, this probe was lysosomal and was suitable for ratiometric detection of intracellular hydrazine in HeLa cells. In addition, trace amount of hydrazine in river and drinking sample can be detected by the probe **45**.

In 2013 Goswami and coworkers[87] reported a carbazole based malonitrile probe **46**, which serve as a ratiometric sensor exclusively for hydrazine via ICT mechanism (Figure 28). This

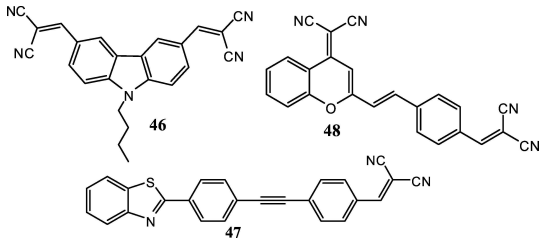

Figure 28. Structures of hydrazine probes **46–48**.

probe shows absorption band at 405, 324 and 258 nm in CH_3CN–H_2O (8 : 2, v/v, pH = 7.4) solution. Upon addition of hydrazine, caused a noticeable decrease of the absorption intensity at 405 nm, accompanied by an enhancement of absorption band at 258 nm and a remarkable color changes from yellow to colorless. In addition, the free probe exhibited weak fluorescence at 356 and 458 nm. The gradual addition of hydrazine into the organo aqueous solution of **46** caused a change in the wavelength of emission maximum from 458 to 413 nm with a noticeable emission color change from light yellow to sky blue. It was verified that the sensing behavior of **46** toward hydrazine was not interfered in presence of various cations and anions such as Ag^+, Cd^{2+}, Co^{2+}, Cu^{2+}, Fe^{3+}, Mn^{2+}, $Na+$, Pd^{2+}, Zn^{2+}, Cl^-, Br^-, I^-, ClO_4^-, SO_3^{2-}, SO_4^{2-} and HPO_4^{2-}. The authors also prepared a test kit for selective detection of hydrazine in water samples.

Another hydrazine specific probe, **47** was described by Qian et al.[88] The maximal absorption of the probe **47** exhibited a blue shift from 395 to 368 nm upon gradual addition of hydrazine (Figure 28). However, fluorescence intensity of this probe in THF/water (1:1) solution was very low but showed drastic fluorescent enhancement at 423 and 480 nm respec-

tively in presence of 12 equivalents hydrazine. In addition, the sensing ability of the probe to hydrazine was not interfered by other biologically and environmentally important ions. This probe showed a very low detection limit of 3.4 nM (0.11 ppb) and worked well over a wide linear range of 60–120 nM.

A novel NIR ratiometric fluorescent probe **48**, bearing a dicyanovinyl group, was reported for the nanomolar detection of hydrazine over other anions and biothiols (Figure 28).[89] Probe **48** exhibited an emission band at 532 nm in DMSO/H_2O solution (4:1 v/v, 10 mM PBS buffer pH = 7.4) when excited at 460 nm. Upon gradual addition of hydrazine, a decrease in fluorescence intensity at 532 nm was observed, accompanied by a remarkable fluorescence enhancement at 660 nm. The reaction of hydrazine with probe **48** induced the conversion of dicyanovinyl group to hydrazone group, thereby enabling ICT process and shifting the weak emission to a strong red emission. The detection limit of this probe for hydrazine was 7.71 nM. Additionally, probe **48** was successfully applied in living cell imaging and also hydrazine detection in real water samples.

Yang's group[90] reported an ICT based colorimetric and ratiometric probe **49**, which consists of an electron acceptor malonitrile group and electron donating phenothiazine dye. The probe **49** in DMF-H_2O (7:3) showed absorption peak at 475 and a very weak emission peak at 490 nm, which was mainly due to the intramolecular charge transition in the molecule. Upon addition of hydrazine, probe **49** was converted to hydrazone product (**49a**) (Figure 29), which disturbed the pi

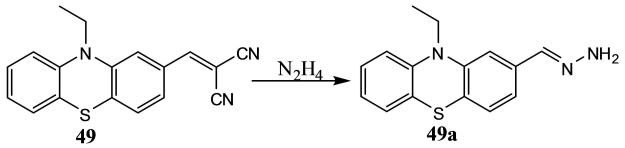

Figure 29. Reactions of probe **49** with hydrazine.

conjugation and influenced the intramolecular electron density distribution, resulting in the enhancement of fluorescence and absorption spectra. The author proved that their probe was membrane permeable and also able to detect hydrazine in living cells. Moreover, this probe was applied for the visual detection of hydrazine in live animals like Zebra fish. The author also reported portable chemosensor kit for hydrazine.

More recently, the ratiometric fluorescent probe **50**, was reported for the sensitive and selective detection of hydrazine over other various biologically important common cations, anions and amines by exploiting ICT mechanism.[91] Upon addition of hydrazine (0–1.2 equiv.) to the solution of **50** in H_2O/CH_3CN (99.5: 0.5, v/v) buffered with HEPES, pH = 7.2, the initial absorption band of probe **50** at 497 nm gradually decreased, with a concomitant increase in a new blue shifted absorption band at 345 nm and the color of the solution changed from red to colorless, allowing a 'naked eye' detection of hydrazine. On excitation at 400 nm, probe **50** showed an emission band centred at 582 nm, resulting from the intramolecular charge transfer from the nitrogen atom of the dimethylamino moiety to electron withdrawing cyano moieties (Figure 30). However, its reaction with hydrazine generated

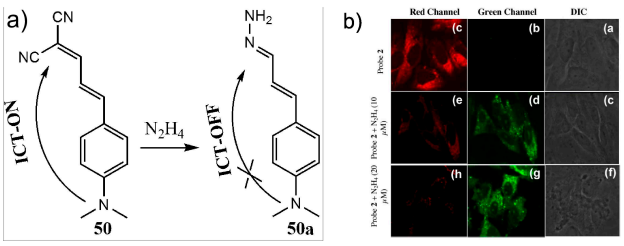

Figure 30. a) Reactions of probe **50** with hydrazine. b) Fluorescence microscopic images of PC3 cell lines. (a–c) cells treated with probe **50** (1 μM) only, (c-e) after incubation with **50** and hydrazine (10 μM), (f-h) after incubation with **50** (5 μM) and then hydrazine (20 μM). Fluorescence images are recorded at green (500 ± 20 nm) and red channels (570 ± 20 nm); λ_{ex} = 405 nm. Reprinted from Ref.,[91] Copyright (2016), with permission from Elsevier.

compound **50** with a maximum emission at 480 nm. The development of an emission band at 480 nm was mainly due to the inhibition of charge transfer from nitrogen atom of the dimethylamino to the amino moiety. The ratio of fluorescence intensities at the two wavelengths (I_{480nm}/I_{582nm}) showed 126-fold in the product (**50a**) relative to the probe **50**. The detection limit of **50** for sensing hydrazine was evaluated to be 8.87 nM, which is considerably lower than TLV (10 ppb) allowed by EPA. The authors reported that reaction between probe **50** and hydrazine was fast at higher temperature. The rate constant (k at 25 °C) under first order reaction conditions was calculated to be $2.63 \times 10^{-3} s^{-1}$. The reactions of **50** with hydrazine were confirmed by ^{1}H NMR, mass spectroscopy and density functional theory calculations. Moreover, the authors reported test kit experiments for the detection of trace amount of hydrazine in environmental samples. Again, probe **50** could be used as a ratiometric fluorescent probe for the bioimaging of hydrazine in living PC3 cell.

An analogous approach was reported by Upadhyay and coworkers.[92] They developed a colorimetric and ratiometric fluorescent probe **51** based on an ICT strategy for the sensitive detection of hydrazine (Figure 31). With the addition of hydrazine, the absorption peak showed a 26 nm blue-shift and the color of the solution turned from yellow to colorless. However, in presence of hydrazine, the fluorescence intensity of **51** decreased at 510 nm and a simultaneous increase at 400 nm with a blue shift of 110 nm, accompanied by a color change from green to blue, was observed. Probe **51** also showed excellent selectivity for hydrazine among other analytes such as aniline, hydroxylamine, 4-nitrophenylhydrazine, ammonia, phenyl hydrazine, pyridine, ethylamine, triethylamine, methylamine, urea, ethylenediamine, cysteine, benzyl amine, thiourea, 2, 4- dinitrophenylhydrazine butyl amine, semicarbazide, thiocarbohydrazide, carbohydrazide and etc. Such fluorescence and absorption changes of probe **51** in

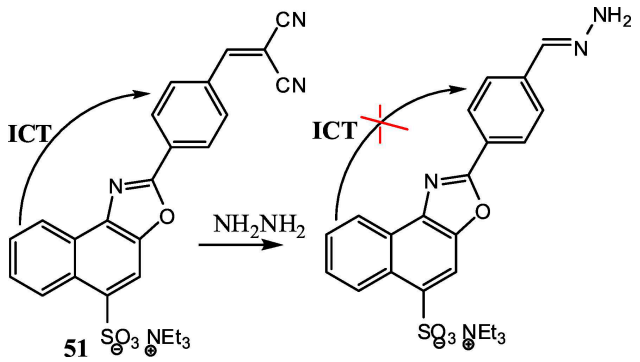

Figure 31. Reaction of probe **51** with hydrazine.

presence of hydrazine was mainly due to the formation of hydrazone moiety followed by the block of ICT process, as confirmed by ^{1}HNMR, ^{13}CNMR, and ESI-MS mass spectra. Furthermore, probe **51** was applied for imaging intracellular hydrazine in HeLa cells using confocal microscopy analysis.

Recently, Zhao et al.[93] described a PET-based turn-on fluorescence probe **52** for sensing of hydrazine (Figure 32). The

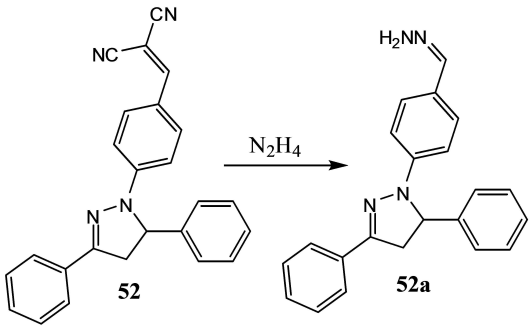

Figure 32. Reaction of probe **52** with hydrazine.

free probe **52** displayed non-fluorescent behavior due to the efficient PET mechanism between electron donor pyrazoline and electron acceptor malonitrile group. However, upon gradual addition of hydrazine to the organo aqueous solution, a remarkable enhancement of emission spectra (λ_{em} = 520 nm, Quantum Yield = 0.010) was observed due to the inhibition of the PET process as a result of the formation of the product **52a** and the color of the solution turned from colorless to green. Moreover, addition of hydrazine to the probe induced a large red-shift of 80 nm in absorption spectra. In addition, they verified that probe **52** could detect hydrazine in several water samples.

The above-mentioned probes for hydrazine detection operate either by an ICT or PET mechanism. But recently, Xie and coworkers[94] reported two 'turn-on' fluorescent probes (**53**) for hydrazine working via TICT (twisted intramolecular charge transfer) mechanism (Figure 33). Initially, probe **53** displayed weak fluoresce in acetonitrile. However, upon addition of

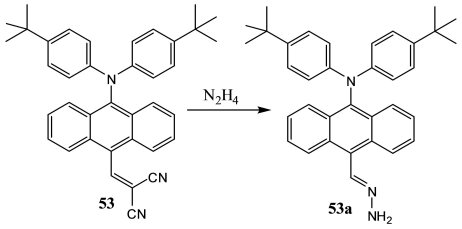

Figure 33. Reactions of probe **53** with hydrazine.

hydrazine, the fluorescence was markedly enhanced due to the formation of fluorescent hydrazone product (**53a**). The formation of this product was confirmed by NMR and mass spectroscopy. Probe **53** exhibited higher selectivity and sensitivity towards hydrazine with a very low detection limit of 7 ppb.

Liu and coworkers[95] developed a series of AIE based probes **54–56** to detect hydrazine in DMSO/H_2O (1/99) solution (Figure 34). For probes **54** and **55**, remarkable color changes

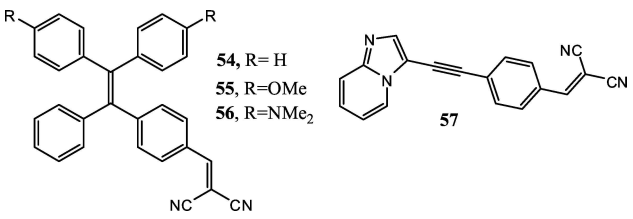

Figure 34. Structures of hydrazine probes **54–57**.

take place from yellow to colorless, whereas **56** exhibits a dramatic color change from red to yellow in the presence of hydrazine. Among the three probes, **56** shows the best response to hydrazine, with a detection limit of 143 ppb in solution. Also, a test paper loaded with probe **56** exhibits fluorescence turn-on from dark to yellow for 1 mM hydrazine solution or 1% hydrazine vapor for naked-eye sensing.

Recently, the analogous approach towards the colorimetric and fluorometric sensing of hydrazine has been revealed by Zhao and co-workers[96] (Figure 34). Using UV-vis spectroscopy, fluorescence spectroscopy and DFT calculations, probe **57** was reported to be the selective and sensitive for hydrazine.

In 2013, Chow's group[97] devised a novel pyridomethane-BF_2 complex probe **58** for selective detection of hydrazine through an internal charge transfer mechanism (ICT) (Figure 35). Probe **58** showed a large 136 nm blue shift to 521 nm along with a 30-fold fluorescence enhancement in presence of 12 equivalents hydrazine. A linear relationship was obtained between the fluorescence intensity and concentration of hydrazine in the range of 4–11 μM. The detection limit for **58** was found to 12 μM. The experimental rate constant of the pseudo-first order reaction of **58** with hydrazine was found to be 0.196 min^{-1} and reaction was completed within 8 min.

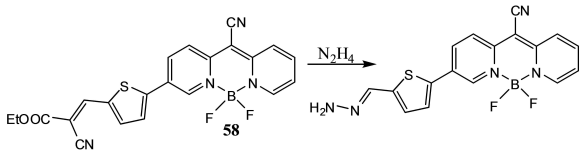

Figure 35. Reaction of probe **58** with hydrazine.

Moreover, this probe was successfully applied to detect hydrazine in solid state.

The colorimetric and ratiometric fluorescent probe **59** was designed for the detection of hydrazine by a hydrazone derivative formation strategy[98] (Figure 36). The probe demonstrated superb selectivity to hydrazine over other competing species such as hydrazine, Cys, Ala, Hcy, GSH, Asp, PhSH, $PhNH_2$, PhOH, Urea, and Thiourea. The detection limits found for hydrazine was 1.6 μM and the limit of quantification (LOQ) value was 0–120 μM. Additionally, probe **59** was reported to be optimal for monitoring hydrazine in living cells.

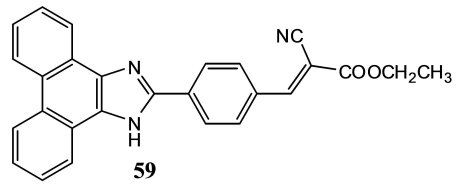

Figure 36. Structures of hydrazine probe **59**.

A new hydrazine selective two photon fluorescent probe **60** based on a naphthalene derivative with 2-benzothiazoleacetonitrile as a recognition site was designed by Lin et al.[99] (Figure 37). It showed selective and sensitive fluorescence enhancement (16-fold) in presence of hydrazine, whereas other comparative analytes including metal ions, anions, reducing agents, small molecule thiols did not exhibit the same response. This probe was applied for the detection of vapor phase hydrazine. Moreover, probe **60** can also be used to detect hydrazine in live HeLa cells as well as in living tissues for the first time.

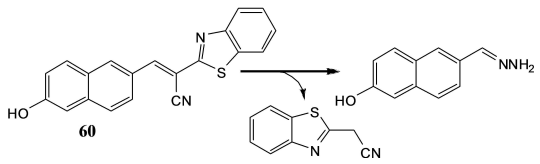

Figure 37. Reaction of probe **60** with hydrazine.

Hydrazone formation is a trademark of hydrazine. Hence the selectivity of probes employing this technique tends to be very good. Electron withdrawing groups such as nitrile when removed from the sensing species after hydrazone formation often lead to ratiometric fluorescence. Also, Knoevenagel condensation reactions are simple to carry out successfully and hence such probes can be synthesized with relative ease.

1.6. Other different approaches

Several strategies have been devised for the design of hydrazine sensors.

1.6.1 Pyrazole forming reaction

Goswami's group reported a coumarin-based fluorescent probe **61** for the detection of hydrazine.[100] The addition of increasing concentrations of hydrazine to acetonitrile solutions of 25 resulted in a decrease in an absorption band at 485 nm and formation of two new hypsochromic absorption band at 445 nm and 395 nm, corresponding to a color change from orange yellow to green. Also, on addition of hydrazine to the solution of **61**, the emission band at 545 nm gradually shifted to 500 nm (a blue-shift of 45 nm), resulting in an emission color change from green to blue. Various amines such as ethylenediamine, dimethylamine, triethylamine, NH_2OH, piperazine, and different biologically important ions did not induce any noticeable visible and spectral changes. As in the above cases, the sensing mechanism was mainly due to the formation of five-membered cyclized product i.e. pyrazole derivative (**61 a**) by the reaction between **61** and hydrazine, as shown in Figure 38. Moreover, the formation of **61 a** was complete with in 180 s with first-order rate constant 20×10^{-3} s^{-1}.

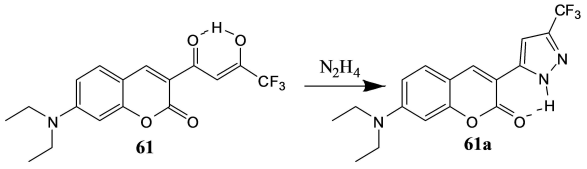

Figure 38. Reactions of probe **61** with hydrazine.

Goswami and coworkers[101] reported another naphthalene based fluorescent probe **62** for the selective detection of hydrazine through the opening of the chromenyl ring via the pyrazole ring formation, as shown in Figure 39. Upon excitation

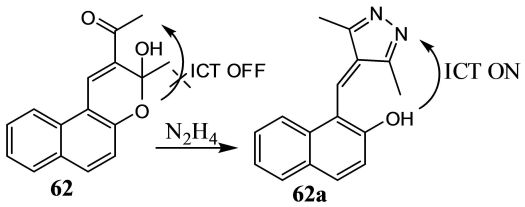

Figure 39. Reactions of probe **62** with hydrazine.

at 327 nm, probe **62** displayed very weak fluorescence (quantum yield = 0.016) in CH_3CN–HEPES buffer (50/50, v/v, pH-7.4), due to the inhibition of ICT process. However, on addition of hydrazine to the solution of **62**, the fluorescence emission was gradually enhanced (twenty-fold) at 420 nm with 48-fold enhancement of quantum yield ($\Phi = 0.774$) and emission color changes from colorless to blue, which could be observed by the naked eye. The authors reasoned that the resulting –OH group in **62a** suffers from a strong ICT due to its large conjugation with the two pyrazole nitrogens and also the basicity of hydrazine. The detection limit of **62** for hydrazine was calculated as 0.22 ppb. In addition, they performed quantum chemical calculations with the B3LYP exchange function, employing B3LYP/6-311+g** basis sets in order to explain the structural and optical properties of this probe. Moreover, the authors also demonstrated the use of probe **62** to detect intracellular hydrazine in Human lung cancer cells (NCI–H460).

Bandyopadhyay and co-workers[102] designed two "turn-on" fluorescent chemodosimeter **63** containing phenanthrene group and **64** containing anthracene group for the intracellular detection of hydrazine (Figure 40). Probe **63** exhibits 83-fold

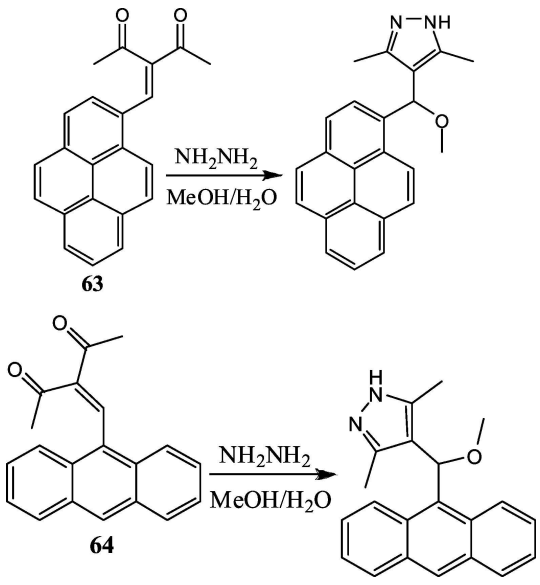

Figure 40. Reactions of probes **63** and **64** with hydrazine.

and probe **64** displays 173-fold emission enhancement in response to hydrazine in H_2O/MeOH (4:1, v/v) solution. The sensing mechanism of these chemodosimeters involves the irreversible reaction of **63** & **64** with hydrazine to produce a reaction intermediate which further undergoes aromatization in presence of methanol to give fluorescence pyrazole moiety. However, these probes did not show any significant change in fluorescence spectra with the addition of excess amounts of other metal ions, anions, nitrogenous organic bases, thiols, and lanthanides, indicating the excellent selectivity of these probes over other competitives. These probes were able to sense solution and vapor phase hydrazine using handy test strips. It was found that probe **63** & **64** was able to detect hydrazine in live Drosophila larvae and in human breast cancer cells.

Xu et al.[103] reported a turn-on fluorescent probe (**65**) for hydrazine imaging in living cells based on PET mechanism (Figure 41). When hydrazine was added to the EtOH/HEPES

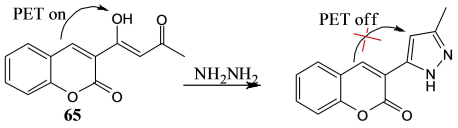

Figure 41. Reactions of probes **65** with hydrazine.

(10 mM, pH = 7.40, 1/1, v/v) solution of probe **65**, a fluorescence maximum appeared at 425 nm (Quantum yield = 0.18) 'naked eye' blue emission of the resulting solution under 365 nm UV lamp. Probe **65** showed an excellent selectivity for hydrazine among a series of cations and anions and its detection limit was 3.2 ppb. Moreover, the sensing mechanism was confirmed by ^{1}H NMR, IR, MS and DFT calculation. It was found that probe **65** could be used to monitor the intracellular hydrazine in glioma cell line U251.

Sessler et al.[104] reported the three-step synthesis of the trifluoroacetyl acetonate naphthalimide derivative **66**, which readily forms five membered cyclic products in presence of hydrazine (Figure 42). Probe **66** showed a weak emission band

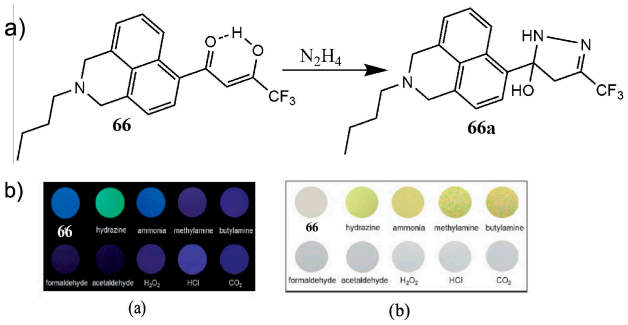

Figure 42. a) Reactions of probe **66** with hydrazine. b) (a) Fluorescent and (b) Visual color changes of probe **66**-coated TLC plates after exposure to an excess quantity of various vapors, including hydrazine, ammonia, methylamine, n-butylamine, formaldehyde, acetaldehyde, H_2O_2, HCl, and CO_2 for 1.0 min, respectively. Reproduced from Ref.[104] with permission of The Royal Society of Chemistry.

centred at 445 nm in CH_3CN. However, its reaction with hydrazine produced compound **66a** with maximum fluorescence intensity at 501 nm and the color of the solution changed from blue to green. The authors confirmed the transformation from reactant (**66**) to product (**66a**) on reaction with hydrazine by ^{1}H NMR and mass spectroscopy. The authors found that the reaction was very much effective under acidic environments and the authors used this probe for the vapor

phase detection of hydrazine, without interferences from other environmentally abundant vapors, such as formaldehyde, acetaldehyde, H_2O_2, HCl, and CO_2. Furthermore, probe **66** was used to selectively image intracellar hydrazine in HeLa cells.

Recently Tang et al.[105] prepared the tetraphenylethene based polymeric fluorescent probe **67** for selective detection of hydrazine in DMF solution (Figure 43). The reaction of

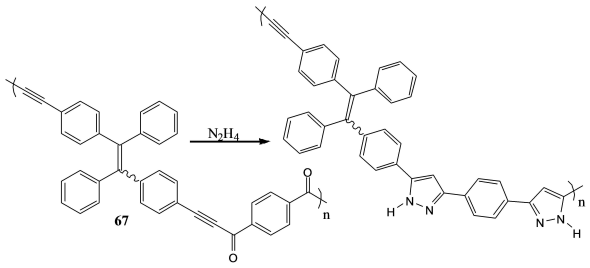

Figure 43. Reactions of probe **67** with hydrazine.

hydrazine with the probe **67** resulted in significant fluorescent enhancement and was associated with a visually detectable change in the solution phase fluorescence from yellow to deep green. The limit of detection for hydrazine was determined to be 2 ppm. The authors also reported the solid-state detection of hydrazine and it was found that the weakly yellow fluorescent filter paper showed strong green emission in presence of hydrazine. Kinetic studies showed that the reaction between probe **67** and hydrazine was complete within 10 min. As above, the response observed was mainly due to the formation of pyrazole unit.

Very recently, Liu et al.[106] designed a chemosensor, composed of an ynone reactive unit (**68**) for detection of hydrazine (Figure 44). Here, inherent carbonyl group present in

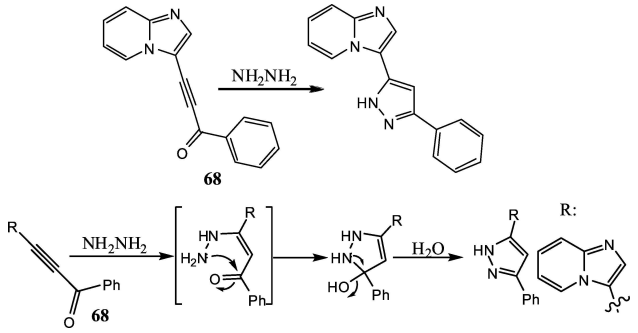

Figure 44. Structure of probe 68 and reaction mechanism of probe **68** with hydrazine.

the probe **(68)** acting as the fluorescent quencher. Reaction with hydrazine the ynone unit is converted to pyrazole moiety, a turn-on response was achieved. TD-DFT calculation also supports the above reaction mechanism. Due to the rapid optical response, the probe **68** is also applied hydrazine real-time detection. The detection limit of hydrazine was calculated to be as low as 0.253 ppb. Importantly, the sensor could be applied for detection of hydrazine both in laboratory and in the marketplace.

Wang et al.[107] have synthesized chalcone-based probe **69** which in presence of hydrazine form highly fluorescent pyrazole derivatives **69** (Figure 45). Detection limit of the probe

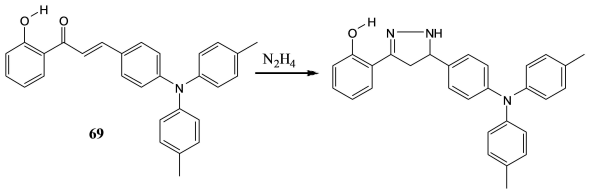

Figure 45. Reaction of probe **69** with hydrazine.

towards hydrazine is below 0.3 μM (9.6 ppb). The application of the fluorescent probe in monitoring hydrazine in living cells and zebrafish embryos were also explored.

1.6.2. Condensation reaction

Probe **70** proved to be an appropriate probe for hydrazine in aqueous solution and living cells (Figure 46).[108] Upon the

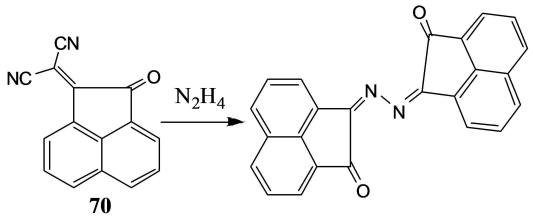

Figure 46. Reaction of probe **70** with hydrazine.

addition of hydrazine to a PBS-CH_3CN (9/1, v/v, pH 7.4) solution of **70**, the emission at 565 nm increased significantly and this fluorescence enhancement resulted in an emission color change from grey to green. The detection limit for hydrazine was determined to be 0.3 μM. This sensor, which displayed a 15.2-fold fluorescent enhancement in the presence of hydrazine, has been utilized to monitor hydrazine in living cells.

1.6.3. Reduction reaction

Liu et al.[109] designed another AIEgen based probe **71**, that was shown to exhibit selective recognition toward hydrazine over other cations (Na^+, K^+, Mg^{2+} and Ca^{2+}), anions (SO_3^{2-}, $S_2O_3^{2-}$, SO_4^{2-} and NO_3^-), amino acids (glycine, aspartic acid, lysine and cysteine), biothiol (GSH), sugar (D-glucose) and protein (BSA). Probe **71** consisted of a fluorescence quencher –N=N- group, which was reduced to –NH–NH– in presence of hydrazine to

give turn on fluorescence signal. As shown in Figure 47, the reduced intermediate can be simply oxidized in air to restore

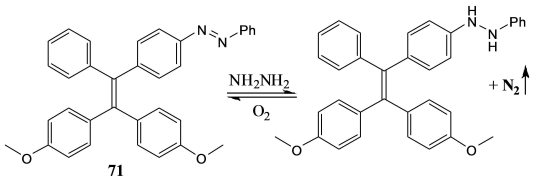

Figure 47. Reaction of probe **71** with hydrazine.

the original probe for recyclable usage. Probe **71** was used to monitor hydrazine in live cells.

1.6.4. Cleavage of the S–O bond

Jiang et al.[110] developed a turn-on fluorescent probe **72** for the selective detection of hydrazine based on the nucleophilic properties of hydrazine. Probe **72** is weakly fluorescent in its unreacted state; on the addition of hydrazine, probe **72** was proficiently converted to a fluorescent 6-acetyl-2-hydroxynaphthalene moiety with a turn-on fluorescent response. Such fluorescent enhancement was attributed to the cleavage of the strong electron-withdrawing 4-nitrobenzenesulfonate group from probe **72** and the release of the fluorophore moiety as shown in Figure 48. Furthermore, cytotoxicity and confocal

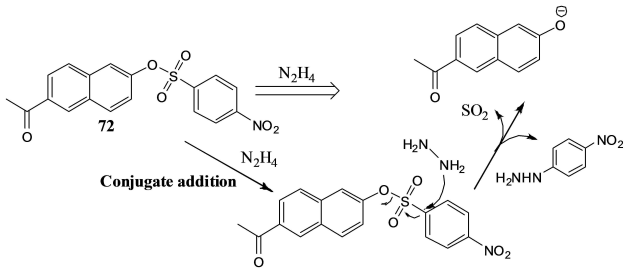

Figure 48. Reaction mechanism of probe **72** with hydrazine.

scanning microscopy experiments indicated that probe **72** had good biocompatibility, cell permeability and was able to image hydrazine in live cells.

1.6.5. Metal ion ensemble hydrazine detection

Zhang group[111] reported probe **73** based on the chemistry of the metal ion reducing ability of hydrazine (Figure 49). Probe **73** displayed fluorescence turn-on response towards Pd^0 over all other comparative metals ions including Pd^{2+} in CH_3CN-PBS (v/v = 1/3, pH = 7.4, 10 mM) solution. Taking the benefit of Pd^0 sensing capability of probe **73** and the metal ion reducing power of hydrazine, Zhang group used this probe as a sensitive sensor for hydrazine. The probe **73** is not itself fluorescent due

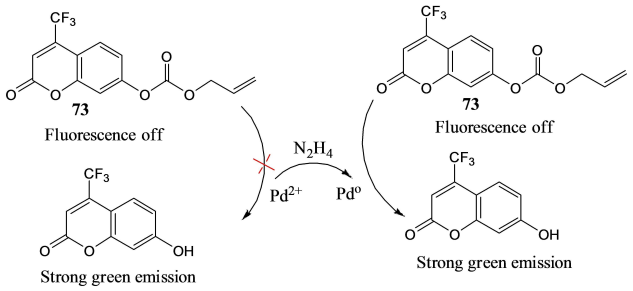

Figure 49. Reactions of probe **73** with hydrazine.

to the presence of allyl formate group, resulting in fluorescence quenching of the coumarin fluorophore. After gradual addition of hydrazine to the mixed solution of **73** (10 μM) and Pd^{2+} (100 μ M), probe **73** displayed a significant fluorescent emission at ~500 nm, which is due to the release of reduced Pd^0 and the fluorescent coumarin moieties by hydrazine. The detection limit for hydrazine was calculated to be 37 nM (~1.2 ppb).

1.6.6. Cleavage of carbon-carbon double bond and amide bonds

Li et al.[112] demonstrated the synthesis and sensing properties of fluorescent probe **74** based on 1,8-Naphthalimde for the detection of hydrazine in living cells (Figure 50). The addition

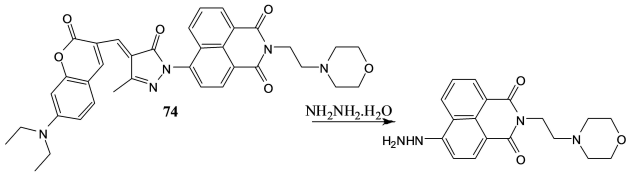

Figure 50. Reaction of probe **74** with hydrazine.

of hydrazine induced fracture of C=C and dissociation of amide with a subsequent 24-times enhancement of emission at 517 nm. To reveal the selectivity of probe **74**, other various species including neutral molecules including Et_3N, $NH_3 \bullet H_2O$, $C_2H_4(NH_2)_2$, thiourea, urea, and aniline, metal ions (Na^+, Mg^{2+}, Al^{3+}, K+, Ca^{2+}, Cr^{3+}, Mn^{2+}, Zn^{2+}, Pt^{2+}, and Pb^{2+}), anions (HPO_4^{2-}, H_2PO^{4-}, SO_4^{2-}, CH_3COO^-, HS^- etc), and nucleophilic biological species (Gly, Gin, GSH, Asp, Cys, Thr, Ala, Phe, Met, Lys, Leu, Ile, Val, Glu, Ser, Arg, Pro, Hcy and Tyr) were examined and all these species showed no apparent change in their fluorescence spectra under the similar conditions. The detection limit was 140 nM under the experimental conditions. Probe **74** was used for the detection of hydrazine in living cells.

1.6.7. Rupture of C=C bond followed by hydrazone formation

Ni and coworkers[113] reported a hemicyanine and coumarin derivatives based NIR fluorescent on-off probe **75** for detection

of hydrazine (Figure 51). This probe itself exhibits two emission peaks centered at 510 nm and 660 nm when excited at

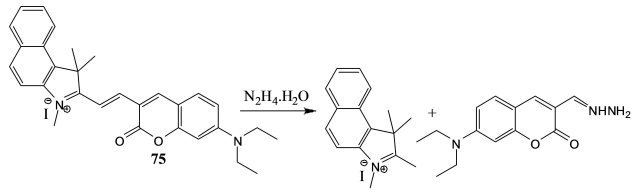

Figure 51. Reaction of probe **75** with hydrazine.

450 nm. However, upon gradual addition of hydrazine, a large fluorescence turn-off response occurs with quenching of emission at 660 nm and the appearance of a new peak at 510 nm with a clear isosbestic point at 633 nm. Under the same experimental conditions, other comparative species did not show any apparent fluorescence change. Moreover, the detection limit of probe **75** was found to be 560 nM, which is responsive enough to detect hydrazine concentrations in a health risk range.

Similar chemistry was developed by Yu group[114] to design carbon nanodots (CDs)-hemicyanine nanohybrid system-based probe **76** which was successfully used for the selective detection of hydrazine in organo-aqueous solution (Figure 52).

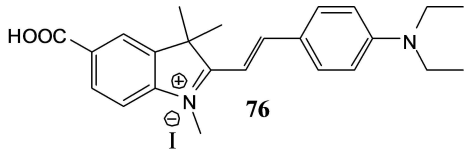

Figure 52. Structure of hydrazine probe **76**.

Probe **76** did not show any significant change in fluorescence spectra with the addition of other comparative species. The detection limit of hydrazine was determined to be 8.0 mM and the limit of quantification (LOQ) was 0–1 mM.

1.6.8.Nucleophilic substitution followed by addition-elimination in aryl ester

Feng et al.[115] reported a new sensing scheme for hydrazine, which was based on a nucleophilic substitution followed by addition-elimination in aryl ester (Figure 53). A 1,8-napthalimide based probe **77** thus undergoes hydrazine promoted reaction to give the subsequent alcohol analogue, the transfer of which gives turn-on fluorescence response and the color of the solution changes from colorless to yellow which could be detect by our naked eye. This mechanism was proved by ^{1}H NMR and mass spectroscopy. The probe **77** showed a fast response to hydrazine (5 min) with a pseudo-first order rate constant (k_{obs}) determined to be about 0.55 min^{-1} and the detection limit was estimated to be 0.10 μM (3 ppb). Probe **77**

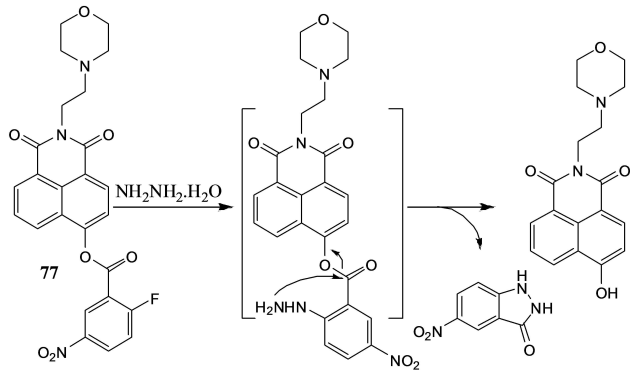

Figure 53. Reaction mechanism of probe **77** with hydrazine.

coated test strips were used to detect vapor/gas phase hydrazine. Moreover, probe **77** was also able to assess intracellular hydrazine in living HeLa Cells.

Utilizing the same tactic, in 2016, Zhou et al.[116] reported a resorufin derivative **78** for the detection of hydrazine in PBS buffer (10 mmol/L, pH 7.4, 30% CH_3CN, v/v) (Figure 54). Free

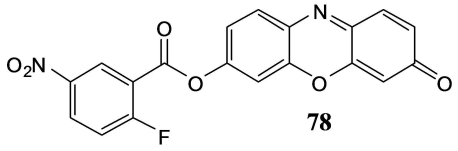

Figure 54. Structure of hydrazine probe **78**.

Probe **78** was weakly fluorescent, but its emission intensity at 589 nm increased with increasing hydrazine concentration. Moreover, upon gradual addition of hydrazine to the PBS-buffer solution of probe **78**, the intensity of absorption band at 456 nm decreased and a new band at 576 nm increased concurrently, resulting a perceived color change from colorless to pink that could be observed by the naked eye. Kinetic studies confirmed that the reaction was complete within 30 min. Compound **78** was used to visualize hydrazine levels in HeLa cells.

1.6.9. Formation of hydrazone followed by cyclization

Commercially accessible compound 2,3-napthalene dicarboxaldehyde (**79**) was designed by Collins et al.[117] as a probe for hydrazine in solution under acidic pH condition (Figure 55). Upon addition of hydrazine to **79** in acidic pH, probe **79** reacted with hydrazine to yield a highly fluorescent product **79a** within 5 minutes. Moreover, probable fluorescence changes in probe **79** were also studied by several competitive species such as cyanide ion, thiol and ammonia but it is found that no reaction occurred in the presence of such analytes.

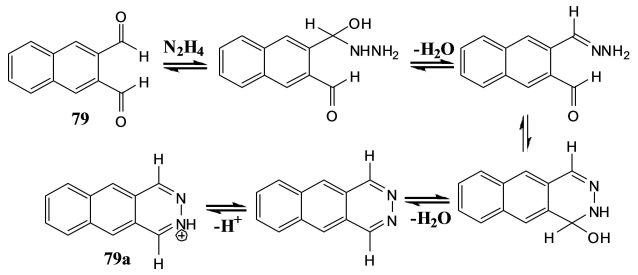

Figure 55. Reaction mechanism of probe **79** with hydrazine.

1.6.10 Cinnamoyl group deprotection strategy

The Nile Red-based probe **80**, possessing a cinnamoyl unit, was fabricated for the detection of hydrazine by Jiang and co-worker[118] (Figure 56). In presence of hydrazine, **80** suffers to a

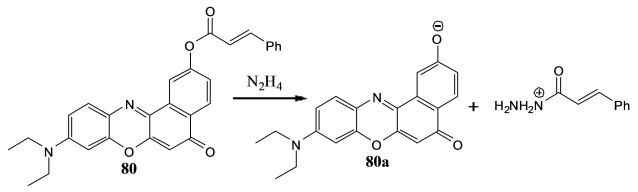

Figure 56. Reaction of probe **80** with hydrazine.

loss of fluorescence emission. This decrease in fluorescence was mainly due to the PET process from the free hydroxyl groups of Nile Red **80a** (Figure 56). Probe **80** illustrated high sensitivity towards hydrazine, with a detection limit of 0.103 μM.

The rhodol-based turn-on fluorescence probe **81** for hydrazine sensing was presented by Kongsaeree and co-workers.[119] The fluorescence intensity of **81** shows a 48-fold enhancement when 300 equivalents of hydrazine is added to aqueous EtOH solution (1:1, v/v, 10 mM HEPES buffer pH 7.4 of **81**. This fluorescence enhancement is attributed to the formation of **81** through the hydrazinolysis and a subsequent ring-opening reaction (Figure 57). Furthermore, **81** was utilized

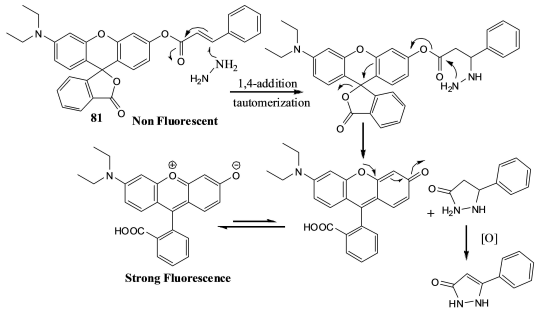

Figure 57. Reaction mechanism of probe **81** with hydrazine.

for intracellular hydrazine imaging in live HepG2 cells using confocal microscopy experiments.

1.6.11. Hydrazone formation

Xu and coworkers[120] reported a series of hydrazine sensor **82–85** that is based on a hydrazone formation reaction strategy (Figure 58). Compound **82** induced an enhancement in

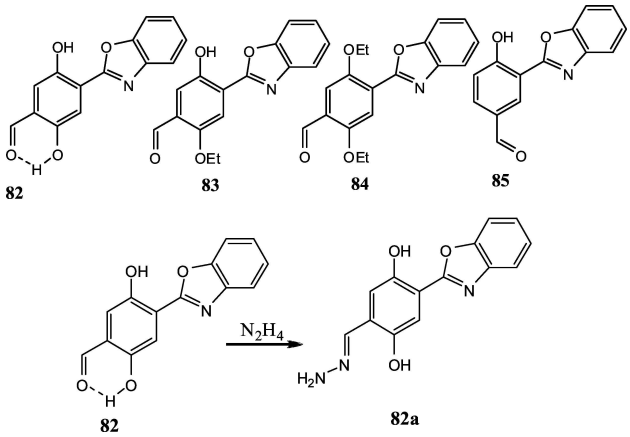

Figure 58. Structures of probe **82–85** and reaction of probe **82** with hydrazine.

fluorescence and UV-Vis spectral changes, which were attributed to formation of hydrazone derivative **82a** in presence of hydrazine in CH_3CN–HEPES buffer (1: 2, v/v, pH 7.4) solution, causing a color change from carnation to yellow-green. Again, kinetic studies showed that the hydrazone formation reaction was complete within about 7 min. Applying UV-vis spectroscopy, fluorescence spectroscopy, ^{1}H NMR titrations and kinetic studies, along with theoretical calculations, probe **82** was reported to be highly selective for hydrazine, with detection limit of 2.7 ppb. Moreover, probe **83–85** did not cause any fluorescence changes; however, it is found that SDS micelles increase the reaction rates of probe **83** to hydrazine.

Another hydrazine sensor that relies on the formation of a hydrazone (**86**) derivative was presented by Zhang and co-workers[121] (Figure 59). The probe exhibited a selective and

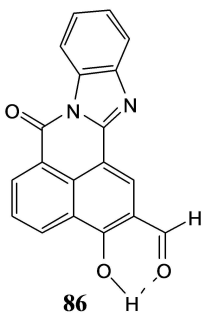

Figure 59. Structure of probe **86**.

sensitive optical response to hydrazine and the detection limit was found to be 0.716 ppb. Moreover, probe **86** coated test strips were able to detect hydrazine vapors in environment.

More recently, Yuan's laboratory[122] designed a spirobenzopyran-based multifunctional sensor **87** which behaved not only as a Cu^{2+}-selective colorimetric sensor but also as a fluorometric turn-off probe in tris-HCl/ethanol (1:1, *v/v*, pH 7.40) buffer solution (Figure 60). Probe **87** was used for quantitative

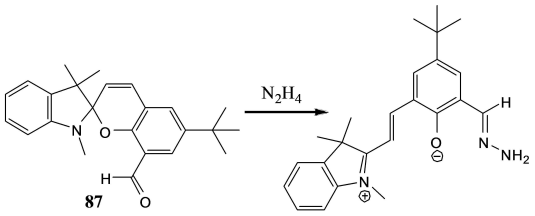

Figure 60. Reaction of probe **87** with hydrazine.

detection of Cu^{2+} and hydrazine in real samples such as pharmaceutical, drinking water, and river water and also qualitative detection of gaseous hydrazine. In addition, Cu^{2+} and hydrazine can also be detected by using **87** containing TLC plates test strip system.

In very recent, Iyer, et al.[123] have developed two novel naphthalimide derivatives and shown that introduction of the formyl group changes an ACQ (Aggregation Caused Quenching) to AIEE (Aggregation Induced Emission Enhancement) which is caused by restriction of intramolecular motion (RIM) (Figure 61).Now, the formylated derivative (**88**) acted as an

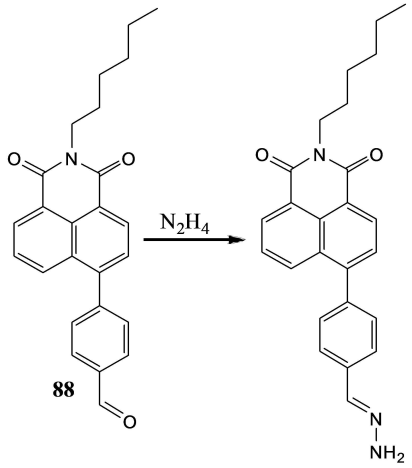

Figure 61. Reaction of probe **88** with hydrazine.

ultrasensitive hydrazine detector at the parts per trillion level (LOD = 81 ppt) in the organo-aqueous solution. The probe can detect hydrazine vapor when immersed in Whatman filter paper (LOD = 0.003%). The detection mechanism involved simple Schiff base formation and quenching in fluorescence intensity. Two mammalian [HeLa (human cervical cancer cell line) and HEK293T (Human embryonic kidney] cell line was used for *in vitro* detection of hydrazine.

1.6.12. Acetyl group deprotection and hydrazone formation in same chromophore

Very recently, Li et al.[124] have synthesized 2-phenyl-benzothiazole based ratiometric fluorescent probe **89** for hydrazine (Figure 62). The probe contains an aldehyde and acetyl group,

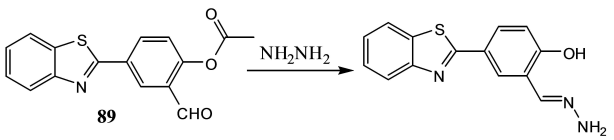

Figure 62. Reaction of probe **89** with hydrazine.

exerts an additive effect in fluorescence spectrum. As the hydroxyl group was blocked by acetyl group, the ICT process was silenced. In presence of hydrazine as the acetyl group was hydrolyzed and the aldehyde group was converted to hydrazone, ICT was restored, responsible for ratiometric fluorescence change. The detection limit of the probe **89** is 2.80 ppb and has found use in intracellular hydrazine detection.

1.6.13. Formation of keto hydrazone followed by cyclization

Yin et al. developed a coumarin based ratiometric fluorescent chemodosimeter **90** for detection of hydrazine in PBS (pH = 7.4) buffer solution.[125] The carbonyl group present in the probe (**90**) initially forms a Schiff base with hydrazine and then forms a stable heterocyclic structure. This type cyclization reaction based on hydrazine detection is first ever reported (Figure 63). The response time of probe towards hydrazine

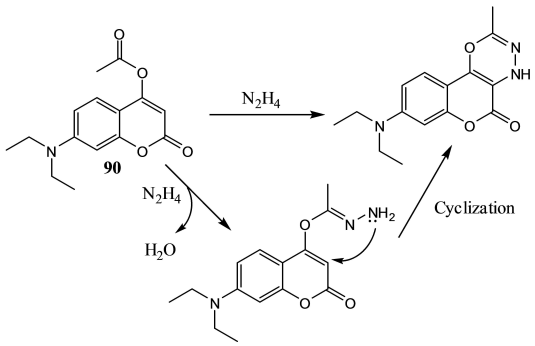

Figure 63. Cyclization reactions of probe **90** with hydrazine.

Table 1. Summary of important properties of hydrazine sensors

Probe	Media	LOD[a]	Application	Ref.[b]
1	DMSO:PBS (1:1, pH 7.4)	0.67 ppb	Detection in (a) real water samples and (b) living cells (7860 cells).	[43]
2	HEPES: CH_3CN(1:1, pH 7.4)	9.40 ± 0.12 nM	Detection in (a) realwater samples;(b) living cells (L929cells), *in vivo* (zebrafish) and (c) vapor phase.	[44]
3–6	DMSO:tris buffer (1:1, pH 8.0)	9×10^{-8} M (3) & 8.2×10^{-7} M (5)	Detection in real water samples by probe 3.	[45]
7	Trisbuffer solution (pH 7.5)	31 nM	Detection in (a) real water, plasma and pharmaceutical samples. (b) vapor phase	[46]
8	acetate buffer :DMSO (1 : 9, pH 4.5)	2×10^{-5} M^{-1}	–	[47]
9	DMSO:H_2O(2:8, pH 7.0)	0.186 μM	–	[48]
10	PBS:DMSO (1:9,pH = 7.4)	–	Detection in living cells (HepG2 cells).	[49]
11	acetate buffer (pH 4.5) and DMSO(1/9, v/v)	0.81 ppb	Detection in (a) real water samples and (b) living cells (MCF-7 cells), living mice.	[50]
12	HEPES buffer (pH 7.4) containing 20% DMSO	0.17 μM (5.4 ppb)	Detection in (a) living cells (HeLa cells), live mouse and (b) vapor phase.	[51]
13	Ethanol/PBS = 5/5, pH = 7.4	5.7×10^{-8} M	(a)Detection in living cells (MCF-7 cells); (b) Detection of hydrazine in solution by test kits.	[52]
14	HEPES buffer (pH 7.4) containing 10% CH_3CN	2.4×10^{-8} M (0.78 ppb)	Detection in living cells (HeLa cells), tissues (rat liver slice) and mice.	[53]
15 & 16	DMSO:H_2O (2:1, pH 7.4)	5.5×10^{-7} M (15) & 4.5 μM (16)	Detection in (a) water samples; (b) living cells (Vero 76 cells), (c) vapor phase. Detection of hydrazine in solution by test kits.	[54]
17	5% DMSO/PBS buffer (pH = 7.4).	4.7×10^{-8} M (0.0474 μM)	Detection in living cells (HeLa cells).	[55]
18 & 19	DMSO:HEPES buffer (pH = 7.4) (9:1, v/v)	0.37 μM (18) and 0.49 μM (19)	Detection in (a) living cells (HeLa cells) and (b) Vapor phase.	[56]
20	B–R buffer (5% ethanol, pH = 7.4)	3.65×10^{-7} M	Detection in living cells (HeLa & 4T-1 cells), living tissues, in vivo studies in mouse.	[57]
21	PBS (pH 8.0) and DMSO (1:5, v/v)	0.016 μM (0.512 ppb)	Detection in living cells (Eca-109 cells).	[59]
22	Acetate buffer (pH 4.5) and DMSO (3:7, v/v)	2.46 μM (0.08 ppm)	–	[60]
23	HEPES: CH_3CN(7:3, pH 7)	2.3ppb	Detection in living cells (HeLa cells), and serum samples.	[61]
24	pH 7.4 HEPES/THF (1:9, v/v)	–	Detection in (a) living cells (CHO cells) and (b) vapor phase.	[62]
25	H_2O:DMSO (3:7, v/v, pH = 7.4)	1.87 μM	Detection in (a) water samples; (b) living cells (Vero 76 cells) and (c) vapor phase.	[63]
26	CH_3CN:H_2O (2:3, v/v, pH = 7.4)	6.6×10^{-8} M (2.2 ppb)	Detection in living cells (*Candida albicans* cells).	[64]
27	CH_3CN:H_2O (1:1, pH = 7.1)	3.881×10^{-8} M	Detection in water samples.	[65]
28	HEPES buffer (pH 7.4, 10% CH_3CN)	~2 μM	Detection in living cells (CHO cells).	[66]
29	PBS (pH 7.4) and DMSO (1:9, v/v)	0.15 μM (4.8 ppb)	Detection in living cells. Vapor phase detection.	[67]
30	DMSO–PBS(9 : 1, pH 7.3)	0.36 μM	Detection in water samples.	[68]
31	HEPES buffer(10 mM, pH 7.4, 10% CH_3CN)	0.27 μM	Detection in (a) real water samples; (b) living cells (A549 cells) and (c) vapor phase.	[69]
32	DMSO-H_2O (1:4, PBS 20 mM, pH 7.4)	0.38 ppb	Detection in living cells (HeLa cells) and *in vivo* studies in mice.	[70]
33	DMSO-H_2O (v:v, 1:19, pH 7.4)	5.09 ppb	Detection in living cells (HeLa cells) and *in vivo* studies in mice.	[71]
34	PBS buffer (pH 7.4) with 1% ethanol	0.147 μM	Detection in living cells (HeLa cells)	[72]
35	Water and DMSO (4 : 6, v/v)	8.8×10^{-9} M (0.3 ppb)	Detection in (a) living cells (HeLa cells) and (b) vapor phase.	[76]
36	H_2O-DMSO solution (4 : 6, v/v, pH 7.4)	2.9 ppb	Detection in (a) water samples, living cells (Vero 76 cells) and (b) vapor phase. Detection of hydrazine in solution by test kits.	[77]
37	0.4 mM TX- 100 in HEPES buffer (10 mM, pH 7.2)	1.5 ppb	Detection in (a) living cells (HepG2 cells) and *in vitro* assay for aminoacylase-1.	[78]
38	H_2O/DMSO (3:7)	3.2 ppb (0.1 μM).	Detection in (a) living cells (HeLa cells) and (b) vapor phase.	[79]
39	PBS buffer (pH 7.4, 30% CH_3CN)	0.0622 μM (1.99 ppb)	Detection in (a) living cells (HeLa cells) and (b) vapor phase.	[80]
40	HEPES buffer (pH 7.0) and DMSO(1/9)	6.01 ppb (1.88×10^{-7} M),	Detection in (a) living cells (HeLa cells) and (b) vapor phase.	[81]
41 & 42	Water/DMSO (1:9, v/v).	1.4 μM (41) & 0.18 μM (42)	–	[82]
43	PBS buffer (pH 7.2) and EtOH (1:9)	4.2 nM	Detection in living cells (HeLa cells).	[83]
44	DMSO-HEPES (1/1, pH = 7.4)	0.057 μM	Detection in (a) water samples and (b) living cells (BT474 cells).	[84]

Table 1. continued

Probe	Media	LOD[a]	Application	Ref.[b]
45	Acetate buffer (pH 3.7)-DMSO (1/9)	0.70 nM	Detection in living cells (HeLa cells).	[86]
46	CH_3CN–H_2O(8: 2, pH 7.4)	1.02 μM	Detection in water samples. Detection of hydrazine in solution by test kits.	[87]
47	THF/water (1:1)	0.11 ppb	–	[88]
48	DMSO/H_2O (4:1, pH 7.4)	7.71 nM	Detection in (a) water samples and (b) living cells, (MCF-7 cells).	[89]
49	DMF–Tris.HCl buffer (7 : 3)	1.2191×10^{-8} M	Detection in living cells (HeLa cells), live zebra fish. Detection of hydrazine in solution by test kits.	[90]
50	H_2O/CH_3CN (99.5:0.5,v/v, pH = 7.2)	8.87 nM	Detection in living cells (PC3 cell lines). Detection of hydrazine in solution by test kits.	[91]
51	Pure PBS buffer (pH = 7.4, 10 mM)	1.79×10^{-9} M	Detection in living cells (HeLa cells). Detection of hydrazine in solution by test kits.	[92]
52	CH_3CN/acetate buffer, (9:1, pH 5.0)	6.16×10^{-6} M	Detection in water samples.	[93]
53	CH_3CN	7 ppb	–	[94]
54–56	DMSO/H_2O (1/99)	214 ppb (54) 145 ppb (55) 143 ppb (56)	Detection of hydrazine in solution by test kits.	[95]
57	–	–	–	[96]
58	Acetate buffer (pH 4.0) and DMSO (1/9)	12 μM	Vapour phase detection by test kits.	[97]
59	Water/DMSO (4:6, v/v)	1.6 μM	Detection in living cells (A549 cells).	[98]
60	PBS/DMSO (2/1, pH 7.4)	–	Detection in (a) living cells (HeLa cells), mouse liver slice and (b) vapor phase.	[99]
61	CH_3CN solution.	3.38×10^{-6} M	Detection of hydrazine in solution by test kits.	[100]
62	CH_3CN: HEPES buffer (50: 50, pH 7.4)	0.22 ppb	Detection in water samples and living cells (Ncl-H460cells). Detection of hydrazine in solution by test kits.	[101]
63 & 64	H_2O/MeOH (4:1, v/v with 1% DMSO, pH 7.4)	5.4 ppb (63) 7.7 ppb (64)	Detection in (a) water samples, (b) living cells (MCF-7cells) and live *Drosophila* Larva.	[102]
65	Buffered EtOH/HEPES (1/1, pH = 7.40) solution	3.2 ppb	Detection in living cells (U251 cells)	[103]
66	H_2O/CH_3CN (v/v, 1: 9)	3.2 ppb (0.1 μM)	Detection in (a) living cells (HeLa cells) and (b) vapor phase	[104]
67	DMF solution	–	Detection of hydrazine in solution by test kits.	[105]
68	IPA-Tris/HCl buffer (pH = 7.4, 1:1,v/v)	0.253 ppb	–	[106]
69	DMSO solution	0.3 μM (9.6 ppb)	Detection in living cells (hNB cells).	[107]
70	PBS–CH_3CN (9/1, v/v, pH 7.4)	0.3 μM	Detection in (a) human blood samples and (b) living cells (BEL-7402 cells).	[108]
71	THF/H_2O (1: 9, v/v)	–	Detection in (a) water samples and (b) living cells (HeLa cells). Detection of hydrazine in solution by test kits.	[109]
72	PBS buffer (10 mM, pH 7.4).	0.716 ppb (22 nM)	Detection in living cells (HeLa cells).	[110]
73	CH_3CN-PBS (v/v = 1/3, pH 7.4, 10 mM).	37 nM (~ 1.2 ppb).	–	[111]
74	HEPES: DMSO (4:6, pH 7.40)	140 nM	Detection in living cells (HeLa cells).	[112]
75	HEPES: DMSO (5:5, pH 7.40)	560 nM	–	[113]
76	DMSO/water (9/1)	8.0 μM	–	[114]
77	PBS buffer (pH 7.4) with 2% CH_3CN (v/v)	0.10 μM (~ 3 ppb)	Detection in (a) living cells (HeLa cells) and (b) vapor phase. Detection of hydrazine in solution by test kits.	[115]
78	PBS buffer (pH 7.4, 30% CH_3CN)	0.84 μmol/L	Detection in living cells (HeLa cells).	[116]
79	H_2O (pH 3.0)	50ng/l (115 ppt)	–	[117]
80	MeOH/H_2O (v/v = 1: 1, pH = 7.0-8.0)	0.103 μM	Detection in living cells (MCF-7 cells).	[118]
81	Aq.EtOH solution (1:1, v/v pH 7.4)	9.6 ppb	Detection in living cells (HepG2 cells).	[119]
82–85	CH_3CN–HEPES buffer (1: 2, v/v, pH 7.4)	8.42×10^{-8} M (2.7ppb) (82)	Detection in (a) living cells (HeLa cells) and (b) vapor phase.	[120]
86	PBS solution (pH = 7.4, PO_4^{3-} = 10 mM, DMSO: H_2O = 1 : 4)	0.716 ppb (22.5 nM)	Detection in (a) living cells (264.7 cells) and (b) vapor phase.	[121]
87	Tris-HCl/ethanol (9:1,*v/v*, pH 7.40) buffer	–	Detection in (a) real water samples; (b) living cells (Hep-1 cells) and (c) vapor phase.	[122]
88	PBS buffer	2.54×10^{-9} M (81 ppt)	Detection in (a) living cells (HeLa & HEK293T cells) and (b) vapor phase.	[123]
89	CH_3OH:H_2O (1/1, v/v, pH = 7.4)	2.80 ppb	Detection in living cells (BT-474 cells).	[124]
90	PBS (pH = 7.4) solution	31 μM.	Detection in living cells (HeLa cells).	[125]

detection was less than 7 min, and LOD is 31 μM. This probe is also applied for detection of hydrazine in live cells.

These approaches more or less draw from the important and successful strategies described earlier. Each approach has its benefits and shortcomings. That is why such an extensive amount of literature has been generated on the subject. Depending on the target environment, a method may be chosen.

The ratiometric approach stands as superior regardless of the mode of chemical reaction. Ratiometric fluorescence is favoured over other modes of chemosensing because of the larger accuracy obtained by the ratio of intensities at two wavelengths instead of just change in intensity at a single wavelength. Many reports highlight the benefits of this process as it leads to a reduction in error obtained due to background fluorescence. These benefits have been proven not just in case of hyrdrazine sensing but other analytes too.[126] From a study of these successful examples we can conclude that ratiometric responses are generally found in cases where the probe itself has some properties that lead to fluorescence most notable among which is conjugation. Upon reaction with an analyte the probe still fluoresces but at a different wavelength. Another approach is the pairing of two fluorophores via a spacer that makes it a candidate for FRET. FRET properties may be altered by the analytes through changes in the structure of the spacer so that the molecule produces fluorescence at appreciable intensity both before and after analyte interaction leading to ratiometric plots.

2. Summary of hydrazine detection

Several fluorescent chemodosimeters for hydrazine (N_2H_4) are summarized in following Table 1.

3. Conclusion

This review strives to comprehensively highlight significant studies that have focused on the development of new fluorescence and colorimetric chemodosimeters for hydrazine. Based on exhaustive literature survey the most successful chemodosimeters rely on six reaction types according to different reaction mechanisms between the receptor and hydrazine. (1) Cleavage of acetoxy group in presence of hydrazine leads to change in optical properties of the receptor is the most general approach of hydrazine detection. (2) In some of the reported examples, an ester protected fluorophore unit has been deprotected in presence of hydrazine, leading to the change in color and fluorescence properties. (3) In some cases, protection-deprotection strategy for the detection of hydrazine were reported through nucleophilic addition-elimination to tandem cyclization on halo esters. (4) Another interesting way for the detection of hydrazine is the preparation of 'Gabriel amine' from phthalimide. In Gabriel amine synthesis process, N-substituted phthalimide is hydrolyzed by acid or base where basic condition hydrolysis step is the rate-limiting step and hence hydrazine had been used for that step for the hydrolysis of phthalimide. (5) In some cases, arylidene-malononitrile group has been utilized for hydrazine detection where arylidenemalononitrile moiety is converted to the hydrazine unit, responsible for change in photophysical properties. (6) There are some other approaches such as cyclization of 1,3-dikto or a conjugated alkyne-keto groups in presence of hydrazine leads to the formation of pyrazole derivatives. In a certain case arylidene malononitrile compounds undergo condensation in presence of hydrazine. Report exists of fluorescence quencher group, –N=N- yielding turn on fluorescence signal upon reduction to –NH–NH– in presence of hydrazine. Cleavage of S–O bond occurred in presence of hydrazine to regenerate the hydroxyl fluorophore moiety, responsible for turn-on fluorescence indication. Another different type of method of hydrazine detection is metal ion ensemble where the metal ion is reduced in presence of hydrazine and the reduced metal then interacts with a reactive center, thereby producing a turn-on response. Other approaches are cleavage of carbon-carbon double bond and amide bonds, hydrazone formation and nucleophilic substitution followed by addition-elimination in aryl ester. In most of the above cases, reactions are attended by color and/or fluorescence changes. As the reactions are accompanied with change in color, monitored by naked eye, in some cases solid protocols have been constructed to serve as ''dip in'' sensors for hydrazine vapor. In addition, some near-infrared (NIR) probes for hydrazine have the exclusive benefit of drawing molecular activity *in vivo/ in vitro* as NIR photons can pierce comparatively deep into tissues with very low background auto-fluorescence and hence producing less injury to biological samples. Importantly, few examples show ratiometric fluorescent behavior towards hydrazine detection. Ratiometric fluorescence probes have a unique character: all data are calculated by using ratio of two wavelengths, which reduces human as well as instrumental errors. In the end we hope that this review will help motivate in the future the design of highly selective, simple NIR and ratiometric fluorescent probes of very low detection limit for hydrazine.

Acknowledgements

We gratefully acknowledge DST-SERB [File No. EMR/2016/006640] for financial support.

Conflict of Interest

The authors declare no conflict of interest.

Keywords: Bioimaging · Colorimetric · Fluorescent Chemodosimeters · Hydrazine · Test Kits

[1] U. Ragnarsson, *Chem. Soc. Rev.* **2001**, *30*, 205–213.
[2] S. Garrod, M. E. Bollard, A. W. Nicholls, S. C. Connor, J. Connelly, J. K. Nicholson, E Holmes, *Chem. Res. Toxicol.* **2005**, *18*, 115–122.
[3] S. D. Zelnick, D. R. Mattie, P. C. Stepaniak, *Aviat. Space Environ. Med.* **2003**, *74*, 1285–1291.
[4] J. A. E. Hannum, Recent developments in the technology of propellant hydrazines.Chemical Propulsion Information Agency; June 1982. CPTR 82–15.

[5] Hydrazine and Its Derivatives, in Kirk-Othmer Encyclopedia of Chemical Technology, ed. J. I. Kroschwitz and A. Seidel, Wiley, New York, 5th edn, 2005, vol. 13, pp. 562–607.
[6] I. C. Vieira, K. O. Lupetti, O. Fatibello-Filho, *Anal. Lett.* **2002**, *35*, 2221–2231.
[7] Y. Y. Liu, I. Schmeltz, D. Hoffmann, *Anal. Chem.* **1974**, *46*, 885–889.
[8] M. Strous, M. S. M. Jetten, *Annu. Rev. Microbiol.* **2004**, *58*, 99–117.
[9] S. Budavari (Ed.), The Merck Index, 12th ed. Merck Research Laboratories, Whitehouse Station, NJ, 1996, p. 816.
[10] G. Choudhary, H. Hansen, *Chemosphere* **1998**, *37*, 801–843.
[11] S. Tafazoli, M. Mashregi, P. J. O'Brien, *J. Toxicol. Appl. Pharmacol.* **2008**, *229*, 94–101.
[12] C. A. Reilly, S. D. Aust, *Chem. Res. Toxicol.* **1997**, *10*, 328–334.
[13] International Agency for Research on Cancer, Reevaluation of some organic chemicals, hydrazine, and hydrogen peroxide. IARC monographs on the evaluation of carcinogenic risk of chemicals to humans, IARC, Lyon, 1999, vol. 71, pp. 991–1013, http://monographs.iarc.fr/ENG/Monographs/vol71/mono71-43.pdf.
[14] U. S. Environmental Protection Agency (EPA), Integrated Risk Information System (IRIS) on Hydrazine/Hydrazine Sulfate,National Center for Environmental Assessment, Office of Research and Development, Washington, DC, 1999.
[15] R.von Burg, T Stout, *J. Appl. Toxicol.* **1991**, *11*, 447–450.
[16] J. Gold, *Nutr. Cancer* **1987**, *9*, 59–66.
[17] E. C. Olson, *Anal. Chem.* **1960**, *32*, 1545–1547.
[18] J. Liu, W. Zhou, T. You, F. Li, E. Wang, S. Dong, *Anal. Chem.* **1996**, *68*, 3350–3353.
[19] N. M. Ratcliffe, *Anal. Chim. Acta* **1990**, *239*, 257–262.
[20] J. R. Stetter, K. F. Blurton, A. M. Valentine, K. A. Tellefsen, *J. Electrochem. Soc.* **1978**, *125*, 1804–1807.
[21] J. R. Wyatt, S. L. Rose-Pehrsson, T. L. Cecil, K. P. Crossman, N. K. Mehta, R. Young, *Am. Ind. Hyg. Assoc. J* **1993**, *54*, 285–292.
[22] H. Bhutani, S. Singh, S. Vir, K. K. Bhutani, R. Kumar, A. K. Chakraborti, K. C. Jindal, *J. Pharm. Biomed. Anal.* **2007**, *43*, 1213–1220.
[23] M. Sun, L. Bai, D. Q. Lui, *J. Pharm. Biomed. Anal.* **2009**, *49*, 529–533.
[24] A. Umar, M. M. Rahman, S. H. Kim, Y.-B. Hahn, *Chem. Commun.* **2008**, 166–168.
[25] H. E. Malone, *Anal. Chem.* **1961**, *33*, 575–577.
[26] X. Chen, Y. Xiang, Z. Li, A. Tong, *Anal. Chim. Acta* **2008**, *625*, 41–46.
[27] M. George, K. S. Nagaraja, N. Balasubramanian, *Talanta* **2008**, *75*, 27–31.
[28] A. P. Demchenko, Introduction to Fluorescence Sensing, Springer: New York, 2008.
[29] J. Li , C. Yin, F. Huo, *RSC Adv.* **2015**, *5*, 2191–2206.
[30] R. P. Haugland, The Handbook: A Guide to Fluorescent Probes and Labelling Technologies, 10th ed.; Molecular Probes: Eugene, OR, 2005.
[31] J. P. Desvergne, A. W. Czarnik, Chemosensors for Ion and Molecule Recognition; Kluwer Academic Publishers: London, 1997.
[32] C. Suksai, T. Tuntulani, *Chem. Soc. Rev.* **2003**, *32*, 192–202.
[33] H. N. Kim, Z. Q. Guo, W. H. Zhu, J. Yoon, H. Tian, *Chem. Soc. Rev.* **2011**, *40*, 79–93.
[34] R. Martínez-Máñez, F. Sancenón, *Chem. Rev.* **2003**, *103*, 4419–4476.
[35] D. G. Cho, J. L. Sessler, *Chem. Soc. Rev.* **2009**, *38*, 1647–1662.
[36] T. Q. Duong, J. S. Kim, *Chem. Rev.* **2010**, *110*, 6280–6301.
[37] X. Q. Chen, Y. Zhou, X. J. Peng, J. Y. Yoon, *Chem. Soc. Rev.* **2010**, *39*, 2120–2135.
[38] X. Q. Chen, X. Z. Tian, I. Shin, J. Y. Yoon, *Chem. Soc. Rev.* **2011**, *40*, 4783–4804.
[39] A. W. Czarnik, Fluorescent Chemosensors for Ion and Molecule Recognition; ACS: Washington, DC, 1992.
[40] M.-Y. Chae, A. W. Czarnik, *J. Am. Chem. Soc.* **1992**, *114*, 9704–9705.
[41] V. Dujols, F. Ford, A. W. Czarnik, *J. Am. Chem. Soc.* **1997**, *119*, 7386–7387.
[42] L. -Y. Niu, Y. -Z. Chen, H. -R. Zheng, L. –Z. Wu, C.-H. Tung, Q.-Z. Yang, *Chem. Soc. Rev.* **2015**, *44*, 6143–6160.
[43] Y Sun, D. Zhao, S. Fan, L. Duan, *Sens. Actuators, B* **2015**, *208*, 512–517.
[44] X. Xia, F. Zeng, P. Zhang, J. Lyu, Y. Huang, S. Wu, *Sens. Actuators, B* **2016**, *227*, 411–418.
[45] M. G. Choi, J. O. Moon, J. Bae, J. W. Lee, S.-K. Chang, *Org. Biomol. Chem.* **2013**, *11*, 2961–2965.
[46] D.-Y. Qu, J.-L. Chen, B. Di, *Anal. Methods* **2014**, *6*, 4705–4709.
[47] K. Li, H.-R. Xu, K.-K. Yu, J.-T. Hou, X.-Q. Yu, *Anal. Methods* **2013**, *5*, 2653–2656.
[48] H. Tse, Q. Li, S. Chan, Q. You, A. W. M. Lee, W. Chan, *RSC Adv.* **2016**, *6*, 14678–14681.
[49] Y.-Z. Ran, H.-R. Xu, K. Li, K.-K. Yu, J. Yang, X.-Q. Yu, *RSC Adv.* **2016**, *6*, 111016–111019.
[50] C. Hu, W. Sun, J. Cao, P. Gao, J. Wang, J. Fan, F. Song, S. Sun, X. Peng, *Org. Lett.* **2013**, *15*, 4022–4025.
[51] J. Zhang, L. Ning, J. Liu, J. Wang, B. Yu, X. Liu, X. Yao, Z. Zhang, H. Zhang *Anal. Chem.* **2015**, *87*, 9101–9107.
[52] J. Ma, J. Fan, H. Li, Q. Yao, J. Xia, J. Wang, X. Peng, *Dyes Pigm.* **2017**, *138*, 39–46.
[53] S. Wang, S. Ma, J. Zhang, M. She, P. Liu, S. Zhang, J. Li, *Sens. Actuators, B* 2018, 261, 418–424.
[54] A. K. Mahapatra, P. Karmakar, S. Manna, K. Maiti, D. Mandal, *J. Photochem. Photobiol., A* **2017**, *334*, 1–12.
[55] Z. Zhang, Z. Zhuang, L. L. Song, X. Lin, S. Zhang, G. Zheng, F. Zhan, *J. Photochem. Photobiol. A* **2018**, *358*, 10–16.
[56] C. Liu, F. Wang, T. Xiao, B. Chi, Y. Wu, D. Zhu, X. Chen, *Sens. Actuators, B* **2018**, *256*, 55–62.
[57] X. Kong, B. Dong, C. Wang, N. Zhang, W. Song, W. Lin, *J. Photochem. Photobiol., A* **2018**, *356*, 321–328.
[58] P. P. Geurink, B. I. Florea, N. Li, M. D. Witte, J. Verasdonck, C.-L. Kuo, G. A. van der Marel, H. S. Overkleeft, *Angew. Chem. Int. Ed.* **2010**, *49*, 6802–6805.
[59] Z. Ju, D. Li, D. Zhang, D. Li, C. Wu, Z. Xu, *J Fluoresc* **2017**, *27*, 679–687.
[60] M. G. Choi, J. Hwang, J. O. Moon, J. Sung, S.-K. Chang, *Org. Lett.* **2011**, *13*, 5260–5263.
[61] S. Zhu, W. Lin, L. Yuan, *Anal. Methods* **2013**, *5*, 3450–3453.
[62] S. Yu, S. Wang, H. Yu, Y. Fenga, S. Zhang, M. Zhu, H. Yin, X. Meng, *Sens. Actuators, B* **2015**, *220*, 1338–1345.
[63] A. K. Mahapatra, R. Maji, K. Maiti, S. K. Manna, S. Mondal, S. S. Ali, S. Manna, P. Sahoo, S. Mandal, M. R. Uddin, D. Mandal, *RSC Adv.* **2015**, *5*, 58228–58236.
[64] S. Goswami, S. Das, K. Aich, B. Pakhira, S. Panja, S. K. Mukherjee, S. Sarkar, *Org. Lett.* **2013**, *21*, 5412–5415.
[65] S. Goswami, K. Aich, S. Das, S. B. Roy, B. Pakhira, S. Sarkar, *RSC Adv.* **2014**, *4*, 14210–14214.
[66] Y. Qian, J. Lin, L. Han, L. Lin, H. Zhu, *Biosens. Bioelectron.* **2014**, *58*, 282–286.
[67] X. Jin, C. Liu, X. Wang, H. Huang, X. Zhang, H. Zhu, *Sens. Actuators, B* **2015**, *216*, 141–149.
[68] X. Zhang, C. Shi, P. Ji, X. Jin, Ji. Liu, H. Zhu, *Anal. Methods* **2016**, *8*, 2267–2273.
[69] Y. Hao, Y. Zhang, K. Ruan, W. Chenb, B. Zhou, X. Tan, Y. Wang, L. Zhao, G. Zhang, P. Qu, M. Xu, *Sens. Actuators, B* **2017**, *244*, 417–424.
[70] Z. Lu, W. Fan, X. Shi, Y. Lu, C. Fan, *Anal. Chem.* **2017**, *89*, 9918–9925.
[71] Z. Lu, X. Shi, Y. Ma, W. Fan, Y. Lu, Z. Wang, C. Fan, *Sens. Actuators, B* **2018**, *258*, 42–49.
[72] J. Zhou, R. Shi, J. Liu, R. Wang, Y. Xu, X. Qian, *Org. Biomol. Chem.* **2015**, *13*, 5344–5348.
[73] S. Gabriel, *Ber. Dtsch. Chem. Ges.* **1887**, *20*, 2224–2236.
[74] M. S. Gibson, R. W. Bradshaw, *Angew. Chem., Int. Ed. Engl.* **1968**, *7*, 919–930.
[75] H. R. Ing, R. H. F. Manske, *J. Chem. Soc., Abstracts* **1926**, 2348–2351.
[76] L. Cui, Z. Peng, C. Ji, J. Huang, D. Huang, J. Ma, S. Zhang, X. Qian, Y. Xu, *Chem. Commun.* **2014**, *50*, 1485–1487.
[77] R. Maji, A. K. Mahapatra, K. Maiti, S. Mondal, S. S. Ali, P. Sahoo, S. Mandal, Md. R. Uddin, S. Goswami, C. K. Quah, H. K. Fun, *RSC Adv.* **2016**, *6*, 70855–70862.
[78] F. Ali, H. A. Anila, N. Taye, D. G. Mogare, S. Chattopadhyay, A. Das, *Chem. Commun.* **2016**, *52*, 6166–6169.
[79] L. Cui, C. Ji, Z. Peng, L. Zhong, C. Zhou, L. Yan, S. Qu, S. Zhang, C. Huang, X. Qian, Y. Xu, *Anal. Chem.* **2014**, *86*, 4611–4617.
[80] L. Wang, F.-Y. Liu, H.-Y. Liu, Y.-S. Dong, T.-Q. Liu, J.-F. Liu, Y.-W. Yao, X.-J. Wan, *Sensors and Actuators B* **2016**, *229*, 441–452.
[81] X. -X. Zhao, J. -F. Zhang, W. Liu, S. Zhou, Z. –Q. Zhou, Y. –H. Xiao, G. Xi, J.-Y. Miao, B. -X. Zhao, *J. Mater. Chem. B* **2014**, *2*, 7344–7350.
[82] B. Li, Z. He, H. Zhou, H. Zhang, W. Li, T. Cheng, G. Liu, *Dyes Pigm.* **2017**, *146*, 300–304.

[83] M. V. R. Raju, E. C. Prakash, H.-C. Chang, H.-C. Lin, *Dyes Pigm.* **2014**, *103*, 9–20.
[84] W. –Z. Xu, W.-Y. Liu, T. -T. Zhou, Y. -T. Yang, W. Li, *Spectrochim. Acta A* **2018**, *193*, 324–329.
[85] H. Falk, A. F. Vaisburg, *Monatsh. Chem.* **1994**, *125*, 549–551.
[86] J. Fan, W. Sun, M. Hu, J. Cao, G. Cheng, H. Dong, K. Song, Y. Liu, S. Sun, X. Peng, *Chem. Commun.* **2012**, *48*, 8117–8119.
[87] S. Goswami, S. Paul, A. Manna, *RSC Adv.* **2013**, *3*, 18872–18877.
[88] Y. Tan, J. Yu, J. Gao, Y. Cui, Y. Yang, G. Qian, *Dyes Pigm.* **2013**, *99*, 966–971.
[89] X. Yang, Y. Liu, Y. Wu, X. Ren, D. Zhang, Y. Yea, *Sens. Actuators, B* **2017**, *253*, 488–494.
[90] M. Sun, J. Guo, Q. Yang, N. Xiao, Y. Li, *J. Mater. Chem. B* **2014**, *2*, 1846–1851.
[91] S. I. Reja, N. Gupta, V. Bhalla, D. Kaur, S. Arora, M. Kumar, *Sensors and Actuators B* **2016**, *222*, 923–929.
[92] Shweta, A. Kumar, Neeraj, S. K. Asthana, A. Prakash, J. K. Roy, I. Tiwari, K. K. Upadhyaya, *RSC Adv.* **2016**, *6*, 94959–94966.
[93] X.-X. Zheng, S.-Q. Wang, H.-Y. Wang, R.-R. Zhang, J.-T. G. Liu, B.-X. Zhao, *Spectrochim. Acta A* **2015**, *138*, 247–251.
[94] B. Chen, X. Sun, X. Li, H. Ågren, Y. Xie, *Sens. Actuators, B* **2014**, *199*, 93–100.
[95] R. Zhang, C.-J. Zhang, Z. Song, J. Liang, R. T. K. Kwok, B. Z. Tang, B. Liu, *J. Mater. Chem. C* **2016**, *4*, 2834–2842.
[96] C. Zhao, C. Huang, S. Yang, H. Chai, Y. Le, L. Liu, *Chem. Lett.* **2017**, *46*, 848–850.
[97] Y.-D. Lin, T. J. Chow, *RSC Adv.* **2013**, *3*, 17924–17929.
[98] Z. Li, W. Zhang, C. Liu, M. Yu, H. Zhang, L. Guo, L. Wei, *Sens. Actuators, B* **2017**, *241*, 665–671.
[99] J.-Y. Wang, Z.-R. Liu, M. Ren, W. Lin, *Sci. Rep.* **2017**, *7*, 42232.
[100] S. Goswami, S. Das, K. Aich, D. Sarkar, T. K. Mondal, *Tetrahedron Lett.* **2014**, *55*, 2695–2699.
[101] S. Goswami, A. K. Das, U. Saha, S. Maity, K. Khanra, N. Bhattacharyya, *Org. Biomol. Chem.* **2015**, *13*, 2134–2139.
[102] B. Roy, S. Halder, A. Guha, S. Bandyopadhyay, *Anal. Chem.* **2017**, *89*, 10625–10636.
[103] W.-N. Wu, H. Wu, Y. Wang, X.-J. Mao, X.-L. Zhao, Z.-Q. Xu, Y.-C. Fan, Z. -H. Xu, *Spectrochim. Acta A* **2018**, *188*, 80–84.
[104] M. H. Lee, B. Yoon, J. S. Kim, J. L. Sessler, *Chem. Sci.* **2013**, *4*, 4121–4126.
[105] J. Li, J. Liu, J. W. Y. Lam, B. Z. Tang, *RSC Adv.* **2013**, *3*, 8193–8196.
[106] L. Liu, Y. Le, M. Teng, Z. Zhou, D. Zhang, C. Zhao, J. Cao, *Dyes Pigm.* **2018**, *151*, 1–6.
[107] Z. Luo, B. Liu, T. Qin, K. Zhu, C. Zhao, C. Pan, L. Wang, *Sens. Actuators, B* **2018**, *263*, 229–236.
[108] J. Zhao, Y. Xu, H. Li, A. Lu, S. Sun, *New J. Chem.* **2013**, *37*, 3849–3852.
[109] X. Cheng, R. Zhang, X. Cai, B. Liu, *J. Mater. Chem. B* **2017**, *5*, 3565–3571.
[110] W. Chen, W. Liu, X.-J. Liu, Y.-Q. Kuang, R.-Q. Yu, J.-H. Jiang, *Talanta* **2017**, *162*, 225–231.
[111] Y. Ding, S. Zhao, Q. Wang, X. Yu, W. Zhang, *Sens. Actuators, B* **2018**, *256*, 1107–1113.
[112] B. Shi, Y. He, P. Zhang, Y. Wang, M. Yu, H. Zhang, L. Wei, Z. Li, *Dyes Pigm.* **2017**, *147*,152-159.
[113] Y. He, Z. Li, B. Shi, Z. An, M. Yu, L. Wei, Z. Ni, *RSC Adv.* **2017**, *7*, 25634–25639.
[114] Z. An, Z. Li, Y. He, B. Shi, L. Wei, M. Yu, *RSC Adv.* **2017**, *7*, 10875–10880.
[115] Q. Zhai, W. Feng, G. Feng, *Anal. Methods* **2016**, *8*, 5832–5837.
[116] T. Tang, Y.-Q. Chen, B.-S. Fu, Z.-Y. He, H. Xiao, F. Wu, J.-Q. Wang, S.-R. Wang, X. Zhou, *Chin. Chem. Lett.* **2016**, *27*, 540–544.
[117] G. E. Collins, S. L. Rose-Pehrsson, *Anal. Chim. Acta* **1993**, *284*, 207–215.
[118] X.-D. Jiang, J. Guan, H. Bian, Y. Xiao, *Tetrahedron Lett.* **2017**, *58*, 2351–2354.
[119] K. Tiensomjitr, R. Noorat, K. Wechakorn, S. Prabpai, K. Suksen, P. Kanjanasirirat, Y. Pewkliang, S. Borwornpinyo, P. Kongsaeree, *Spectrochim. Acta A* **2017**, *185*, 228–233.
[120] L. Xiao, J. Tu, S. Sun, Z. Pei, Y. Pei, Y. Pang, Y. Xu, *RSC Adv.* **2014**, *4*, 41807–41811.
[121] J. Cui, G. Gao, H. Zhao, Ya. Liu, H. Nie, X. Zhang, *New J. Chem.* **2017**, *41*, 11891–11897.
[122] G. Yu, Y. Cao, H. Liu, Q. Wu, Q. Hu, B. Jiang, Z. Yuan, *Sens. Actuators, B* **2017**, *245*, 803–814.
[123] N. Meher, S. Panda, S. Kumar, P. K. Iyer, *Chem. Sci.* **2018**, *9*, 3978–3985.
[124] W. Xu, W. Liu, T. Zhou, Y. Yang, W. Li, *J. Photochem. Photobiol. A* **2018**, *356*, 610–616.
[125] X. Shi, F. Huo, J. Chao, C. Yin, *Sens. Actuators, B* **2018**, *260*, 609–616.
[126] M. H. Lee, J. S. Kim, J. L. Sessler, *Chem. Soc. Rev.* **2015**, *44*, 4185–4191.

Submitted: November 27, 2018
Accepted: June 4, 2019